THE RESPONSE OF BITUMINOUS MIXTURES TO DYNAMIC AND STATIC LOADS USING TRANSFER FUNCTIONS

OCTOBER 1968
NO. 30

by

S. A. SWAMI

Joint Highway Research Project

PURDUE UNIVERSITY
LAFAYETTE INDIANA

Final Report

THE RESPONSE OF BITUMINOUS MIXTURES TO DYNAMIC AND STATIC LOADS USING TRANSFER FUNCTIONS

To: J. F. McLaughlin, Director
Joint Highway Research Project

October 29, 1968

File No.: 2-4-23

From: H. L. Michael, Associate Director
Joint Highway Research Project

Project No: C-36-6W

The attached Final Report "The Response of Bituminous Mixtures To Dynamic and Static Loads Using Transfer Functions" is submitted on the HPR Part II Research Project "Structural Design of Bituminous Mixtures". The report has been authored by Mr. S. A. Swami, Graduate Instructor in Research, of our staff under the direction of Professors W. H. Goetz and M. E. Harr. Mr. Swami also used the report as his Thesis for the Ph.D. degree.

The research reported herein resulted in several primary results. The applicability of the concept of transfer functions for bituminous concrete was examined and found to be useful in predicting and understanding the behavior of asphaltic concrete.

This report is the final report on this research project; however, one or more technical papers will subsequently be prepared and additional research in the topic area is desirable. The Project anticipates that any such research performed by it will be under a project resulting from subsequent proposals.

The report is presented to the Board for acceptance and will be submitted to the ISHC and the BPR for review, comment and acceptance as completion of the project.

Respectfully submitted,

Harold L. Michael

Harold L. Michael
Associate Director

HLM:rg

cc: F. L. Ashbaucher
W. L. Dolch
W. H. Goetz
W. L. Grecco
G. K. Hallock
M. E. Harr
R. H. Harrell
J. A. Havers
V. E. Harvey
G. A. Leonards
F. B. Mendenhall
R. D. Miles
J. C. Oppenlander
C. F. Scholer
M. B. Scott
W. T. Spencer
H. R. J. Walsh
K. B. Woods
E. J. Yoder

Final Report

THE RESPONSE OF BITUMINOUS MIXTURES TO DYNAMIC AND STATIC LOADS USING TRANSFER FUNCTIONS

by

S. A. Swami
Graduate Instructor in Research

Joint Highway Research Project

File: 2-4-23
Project: C-36-6W

Prepared as Part of an Investivation
Conducted by
Joint Highway Research Project
Purdue University
in cooperation with the

Indiana State Highway Commission
and the

U. S. Department of Transportation
Federal Highway Administration
Bureau of Public Roads

Purdue University

Lafayette, Indiana

October 29, 1968

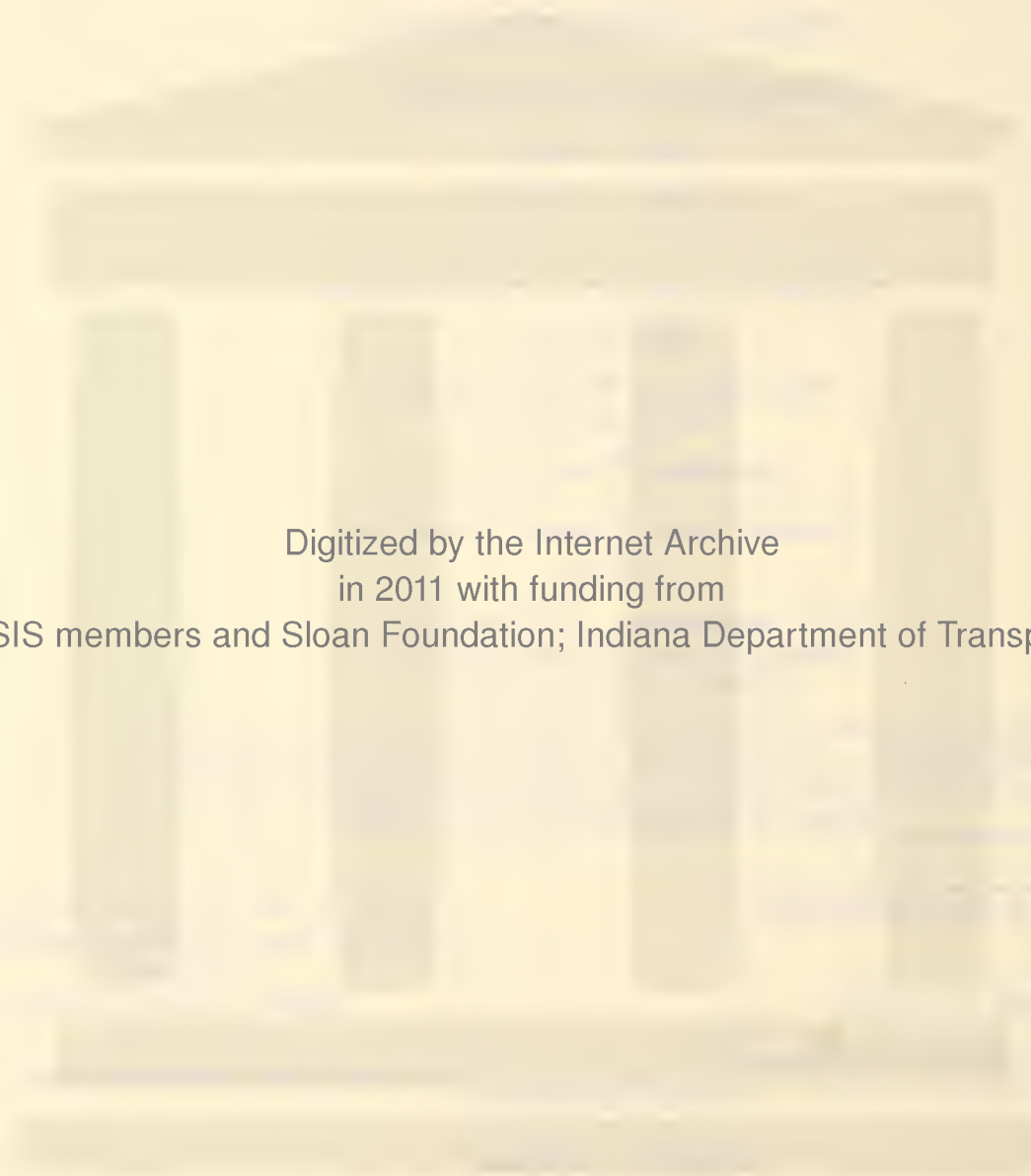

ACKNOWLEDGMENTS

The author is grateful to Professor W. H. Goetz and Professor M. E. Harr, who were the thesis advisors, for their counsel and encouragement.

The author takes this opportunity to thank Mr. R.Vittal Rao, Graduate Assistant in the School of Mathematics, for his useful discussions.

Sincere thanks are extended to the authorities of the Joint Highway Research Project, Engineering Experiment Station, Purdue University in cooperation with the Indiana State Highway Commission and the Bureau of Public Roads, Federal Highway Administration, U.S. Department of Transportation for making available the funds needed for this research.

Special thanks also go the author's wife Anusuya whose patience and understanding aided the successful completion of this investigation.

TABLE OF CONTENTS

TABLE OF CONTENTS (con't.)

LIST OF TABLES

LIST OF FIGURES

LIST OF SYMBOLS

A	-	a constant
a_i	-	root of numerator of transfer function
b_i	-	root of denominator of transfer function
B_i	-	constant coefficient of the differential equation
C_i	-	constants independent of s
e	-	base of natural logarithms
E_1, E_3	-	compression moduli
f_o	-	magnitude of the force input
$f(t)$	-	force input
$\bar{f}(s)$	-	Laplace transform of $f(t)$
G_4	-	shear modulus
$G(s)$	-	Transfer function
$G(j\omega)$	-	modified transfer function
j	-	$\sqrt{-1}$
k_i	-	Slope of the asymptote
K	-	experimental constant
s	-	a complex variable (= $j\omega$)
t	-	time
$x(t)$	-	displacement output
$\bar{x}(s)$	-	Laplace transform of $x(t)$
ϕ	-	phase angle
ω	-	Frequency

$\sigma_1, \sigma_2, \sigma_3$	-	normal stresses
$\sigma_4, \sigma_5, \sigma_6$	-	shearing stresses
$\epsilon_1, \epsilon_2, \epsilon_3$	-	normal strains
$\epsilon_4, \epsilon_5, \epsilon_6$	-	shearing strains
μ	-	Poisson's ratio
db.	-	decibel
oct.	-	octave

ABSTRACT

Swami, Shanmugam Arumuga. Ph.D., Purdue University, January 1969. The Response of Bituminous Mixtures to Dynamic and Static Loads Using Transfer Functions. Major Professor: William H. Goetz.

The applicability of the concept of transfer functions for bituminous concrete has been examined in this study by treating the test specimen as a dynamic system in which the input is the applied force and the output is the resulting displacement. The transfer function was derived from the frequency spectrum of the material using a simple curve fitting technique, and the spectrum itself was obtained from a series of sinusoidal load tests of varying frequencies.

The transfer function derived for the asphaltic concrete was found to be of form

$$G(s) = \frac{A(s + a_1)(s + a_2)(s + a_3)}{(s + b_1)(s + b_2)(s + b_3)(s + b_4)}$$

where s is a complex variable, A is a constant and a_i 's and b_i 's are the roots of the numerator and denominator, respectively. These roots were obtained directly as corner frequencies in the asymptotic approximation of the frequency spectrum.

The scope of the study included dynamic and static testing of specimens of asphaltic concrete of two different compositions, cut along three mutually perpendicular directions from laboratory compacted beams with all testing being carried out at three different temperatures.

The following primary conclusions may be stated as a result of this study:

1. The viscoelastic or time-dependent characteristics of a bituminous concrete can be represented by its transfer function which is unique for the material at a given temperature.

2. The roots of the denominator of the transfer function of the asphaltic concrete tested were observed to be real and distinct which indicates that bituminous concrete behaves as an overdamped system.

3. Temperature is the one single factor which most affects the transfer function for an asphaltic concrete material. Increase in temperature increases the value of the constant A in the transfer function equation.

4. The transfer function is observed to be a powerful tool in predicting the displacement under an applied load, dynamic or static. By treating the static load as a step function of time, the static load displacement was calculated by means of the transfer function derived experimentally from the dynamic test, and compared with the measured static load displacement value. Excellent agreement was noted between the calculated and measured values of the displacements. This validates the concept that the transfer function represents a material property which is independent of the type of input.

5. By the use of the transfer function and without assuming any spring-dashpot model, it is possible to represent the time-dependent behavior of asphaltic concrete by a fourth order linear differential equation with constant coefficients. The coefficients can be computed from the roots of the denominator and numerator of the transfer function.

INTRODUCTION

It is only in recent years that the role of bituminous concrete as a load-distributing layer in flexible pavements has been well recognized, even though it has been used in the upper layers of the pavement for a long time. The results of the AASHO Road test (1)* demonstrated that reduction in pavement deflections and improved performance were effected through the use of asphalt-treated materials in the load-distributing layers. In these applications both the bituminous material and the aggregate serve as structural elements.

Currently used mix design methods (2) employ stability numbers that may provide some measure of quality control but do not relate mixture constituents to loads imposed on the pavement. Further, these methods do not measure any fundamental parameters which can characterize the mechanical behavior of the mixture under a load, static or dynamic, nor do they consider the time-dependent characteristics of the bituminous mixture.

Placed in the top layer of a pavement, the bituminous mix derives its support from the underlying base and subgrade layers and together they form a composite pavement structure. Hence, an essential first step in the rational design of a pavement system is the ability to estimate the stresses and strains induced in its different layers under a given type of loading, at any given time, through a knowledge of the material properties determined from simple laboratory tests that will have significance

---

* Figures in parentheses refer to references in the Bibliography.

under unknown and very complicated field conditions. A necessary second requirement is the availability of some failure criteria, in terms of either stresses or strains for the material of each layer, so that the designer may fix allowable values of these quantities. It is obvious, however, that in the absence of a theory or a method which gives the stresses and strains in a pavement structure, the second requirement cannot be of much practical value.

Use of Elastic Theory

Elastic theory has long been used to investigate the stresses and displacements in layered systems. Solving for the stresses in a pavement, Westergaard (3) assumed the pavement to be a flexible, elastic slab, and the subgrade to act as a series of independent springs. Hogg (4) extended this solution to the case where the top layer is again considered to be a flexible, elastic slab, but where the subgrade is treated as a semi-infinite elastic foundation. A further refinement was introduced by Burmister (5) who solved the problem of the two-layer system by applying the governing equations of elasticity to both layers. He assumed that each layer acts as a continuous, isotropic, homogeneous, linearly elastic medium infinite in horizontal extent. His methods were later extended to cover more than two layers and a wider range of relative thicknesses and material constants (6, 7, 8, 9, 10).

The important consideration in the above discussion is that all of these methods are based on the condition of ideally elastic materials, with fixed elastic constants. That no material is perfectly elastic is generally agreed, and, of course, highway materials are no exception. Under a fast moving wheel load, at freezing temperatures, nearly complete

elastic behavior may be observed. However, the ultimate behavior of a pavement, and particularly of an asphaltic concrete pavement, is obviously nonelastic, since, over a number of years, and under the action of a great many wheel loads, the individually insignificant, nonrecoverable strains accumulate and are felt in many forms, such as rutting in the wheel path, flow in the direction parallel to that of the traffic, or simply as a brittle crack.

Use of Viscoelastic Theory

In order to take into consideration the time dependent response to loads of the pavement materials, they are generally assumed to be linearly viscoelastic. This simplifies their representation and makes analyses less complex. Stress and strain for linear viscoelastic materials can be related by either differential or integral linear operators (11). The differential operator form of the stress-strain law is most commonly used and as Biot (12) has pointed out may be visualized as a combination of springs and dashpots.

For a number of years engineers have recognized that the component materials of a pavement system have time dependent stress-strain properties due to consolidation and creep (13, 14). Layered systems were not, however, analyzed using time dependent (viscoelastic) material properties until after the development of the correspondence principle for isotropic media in 1955 by Lee (11) and shortly thereafter the extension by Biot (15) to include anisotropic media. More general methods of viscoelastic stress analysis have been described by Lee (16) and Lee and Rogers (17).

Viscoelastic layered systems have been solved for only two layers characterized by idealized stress-strain material properties such as those

represented by Maxwell, Voigt, and four element viscoelastic models. Most of these solutions consider a Winkler-type foundation (18, 19, 20, 21), or a system of linear elements with only limited interaction (22, 23, 24).

Monismith and Secor (25) attempted to validate viscoelastic theory for a simple layered system by comparing theoretical predictions of surface deflection with experimental values. The system consisted of a square slab of asphaltic concrete which rested on a bed of closely spaced springs. It was observed that the agreement between the experimental and theoretical deflections was not very good, especially at higher test temperatures.

Perloff and Moavenzadeh (26) presented an analysis for deflection due to a point load moving across the surface of a semi-infinite homogeneous linear viscoelastic medium assuming the response of the material to deviatoric stress to be that of a Kelvin model. Using an N-element Kelvin model, Barksdale and Leonards (27) developed a method for viscoelastic analysis to investigate pavement systems subjected to repeated loadings and found that this method gave a realistic first approximation to the actual behavior of a bituminous pavement system. Harr (28) used a two element model to show the influence of vehicle speed on pavement deflection.

Other models ranging from very simple ones to infinite series of springs and dashpots have been utilized in attempts to explain the time dependent deformations in pavements. To date, however, no single viscoelastic model that would permit accurate prediction of pavement performance has emerged.

Material Coefficients for Transverse Anisotropy

The design of a pavement system, like that of other engineering structures, must start with an understanding of the materials involved. In both the elastic and viscoelastic approaches the asphaltic concrete has been assumed to be homogeneous and isotropic. However, evidence gathered by researchers indicates that bituminous mixtures as used in pavements do not conform to the behavior predicted by the assumption of isotropy. Roscoe and Schofield (29) and others (30, 31) have promoted concepts of anisotropic behavior in soils and bituminous mixtures. Nevitt (32) and Gaudette (33) have shown that particle orientation takes place during compaction of bituminous mixtures. In the pavement, aggregate particles tend to arrange themselves in positions with the long axis horizontal. This preferred orientation is a cause of transversely anisotropic behavior.

Hearmon (34) presented a symmetric matrix established with the aid of strain-energy functions for a homogeneous, elastic, transversely anisotropic material which conserves strain energy. This matrix has five independent coefficients which describe the stress-deformation behavior of such a material.

Recognizing the fact that strain energy is not conserved in bituminous mixtures whose stress-deformation behavior is time dependent, Busching (35) derived a matrix of material coefficients without the use of strain-energy functions. The resulting matrix is nonsymmetric and has six independent coefficients that describe the behavior of a homogeneous, transversely anisotropic, nonconservative material subject to small strains. These coefficients are functions of time and temperature. The

stress-strain constitutive relations in terms of these six material coefficients are as follows:

$$\epsilon_1 = \frac{1}{E_1}\sigma_1 + \frac{\mu_{21}\sigma_2}{E_1} + \frac{\mu_{13}\sigma_3}{E_3} \tag{1}$$

$$\epsilon_2 = \frac{\mu_{21}\sigma_1}{E_1} + \frac{1}{E_1}\sigma_2 + \frac{\mu_{13}\sigma_3}{E_3} \tag{2}$$

$$\epsilon_3 = \frac{\mu_{31}\sigma_1}{E_1} + \frac{\mu_{31}\sigma_2}{E_1} + \frac{1}{E_3}\sigma_3 \tag{3}$$

$$\epsilon_4 = \frac{1}{G_4}\sigma_4 \tag{4}$$

$$\epsilon_5 = \frac{1}{G_4}\sigma_5 \tag{5}$$

$$\epsilon_6 = \frac{2}{E_1}(1 - \mu_{21})\sigma_6 \tag{6}$$

The six material coefficients are easily determined for a given material at a given temperature using uniaxial compression and shear tests as a function of time. Hence, Eqs. 1 through 6 can be used to predict the displacements at any point knowing the stresses at that point. However, from a practical standpoint there are limitations to the use of these equations. Busching evaluated the coefficients over a period of only 30 seconds because it was not possible to evaluate the shear modulus G_4 over longer duration, though it was possible with the other coefficients. Besides, these equations cannot be applied for dynamic loadings. Hence, in a time-dependent analysis, such as in the case of bituminous

mixtures, Eqs. 1 through 6 have limited application.

Transfer Function as a Material Characteristic

It is obvious from the above discussions that none of the current theoretical methods adequately describe the time-dependent response of bituminous mixtures and that there exists a need to find a parameter or parameters or a function which can satisfactorily serve the purpose. Such a function should necessarily be time dependent and should be able to be used as the material characteristic for both static and dynamic loads.

A study of the literature reveals that transfer functions are frequently used to characterize a dynamic system in electrical and mechanical engineering problems (36, 37, 38, 39). The transfer function serves as the link between the time-dependent input and output of the system. A simple example is that of a mechanical system consisting of a spring with a spring constant K, a dashpot with a viscosity coefficient B, and a mass M, subjected to a forcing function f(t) which is the input to the system (39). The differential equation of motion for this system is given by

$$M\ddot{x}(t) + B\dot{x}(t) + Kx(t) = f(t) \qquad (7)$$

where $x(t)$ = output of the system which is the displacement from the position of stable equilibrium;

$\dot{x}(t)$ = velocity of the system with respect to the inertial reference.

$\ddot{x}(t)$ = acceleration of the system.

The transfer function for this system is obtained from the ratio of the Laplace transform of the output $\bar{x}(s)$ to that of the input $\bar{f}(s)$, as

$$G(s) = \frac{\bar{x}(s)}{\bar{f}(s)} \qquad (8)$$

Laplace transform of Eq. 7, neglecting initial conditions, yields the relationship between $\bar{x}(s)$ and $\bar{f}(s)$ as

$$(Ms^2 + Bs + K)\,\bar{x}(s) = \bar{f}(s) \qquad (9)$$

where s is a complex variable. From Eq. 9, the transfer function for the system is seen to be

$$G(s) = \frac{\bar{x}(s)}{\bar{f}(s)} = \frac{1}{Ms^2 + Bs + K} \qquad (9.1)$$

Simple as well as complicated electrical networks are also analyzed through the use of transfer functions to study their frequency responses (36, 39). Also, transfer functions have been successfully used to analyze such diverse dynamical problems as the rolling motion of an airplane (40) on one hand, and the shock and vibration in mechanical systems (41) on the other.

In the light of the above discussion, the transfer function appears to have the potentialities of the function that is needed to study the dynamic response of viscoelastic materials. The present investigation describes a method of obtaining the transfer function for a given bituminous concrete from laboratory tests and studies the extent to which this function can represent the viscoelastic characteristics of the material. Effects of mix type, temperature and anisotropy on the transfer function were studied with a view to providing insight into this function which, it is hoped, may facilitate the development of more refined methods for the structural design of pavements.

TRANSFER FUNCTIONS FOR VISCOELASTIC MATERIALS

The possibility of applying the concept of transfer functions for viscoelastic materials was put forth in the previous section. The means of achieving this and the assumptions involved are discussed in this section.

Concepts of a Mechanical System

The applied stresses due to wheel loads, dynamic or static, and the resulting displacements are the subjects of interest in the case of bituminous mixtures placed in a pavement structure. This is analogous to a mechanical system subjected to a force input and a displacement output. Inasmuch as the dynamical behavior of such a mechanical system can be easily analyzed through transfer functions, it is logical to consider the bituminous mixtures as mechanical systems for the purpose of stress-displacement analysis.

The three fundamental dynamical properties of any mechanical system are inertia, damping and restoring force. These three are represented by the three basic parameters of systems, mass, damping function, and spring function respectively. If the parameters are isolated, then the system is called a lumped-parameter system. To say that the parameters are isolated is to mean that all of the mass of the system is lumped into rigid bodies; all of the damping property of the system is lumped into dampers; and the entire spring-like property of the system is lumped into springs.

However, in actuality, a physically-real spring has mass and is also a damper; a physical damper has mass and some spring-like properties; and a physically real body is deformable and therefore has spring and damping properties. To say that a system is a lumped parameter one is therefore to state an approximation. The dynamical behavior of such a system is described by a second order linear differential equation.

On the other hand, a mechanical system in which the basic parameters are not isolated is called a continuous or distributed-parameter system. The dynamical response of such a system is analyzed through a differential equation of order higher than two which represent the system behavior.

Asphaltic Concrete as a Continuous System

It has been seen from the discussion under "Use of Viscoelastic Theory" that attempts to define the response of bituminous mixtures by the use of spring-dashpot models, that is, by assuming them to be lumped parameter systems, have not yielded satisfactory results. Hence, in this investigation the asphaltic concrete has been analyzed as a continuous mechanical system.

Depending on the degree of damping, such a system can be underdamped, critically damped or overdamped. The nature of the system can easily be recognized through the amplification-frequency plot in a frequency spectrum analysis (41). A distinct peak in the spectrum indicates an underdamped system whereas the absence of a peak and continuous fall of the curve shows an overdamped system.

The frequency spectrums for the asphaltic concrete specimens tested in this investigation indicate an overdamped system.

Analysis of Mechanical Systems Through Transfer Functions

It has been pointed out in the section on "Transfer Function as a Material Characteristic" that transfer functions have been used to analyze the dynamical response of mechanical systems. In those cases where the system behavior is known, the transfer function is easily obtained from the differential equation relating the output and the input variables. However, for systems whose behavior is unknown, the transfer function may be approximated from certain types of input-output data obtained from laboratory tests (36, 39, 41). This method of obtaining the transfer function is followed in the case of asphaltic concrete specimens in this investigation in the absence of any prior knowledge of their dynamical behavior.

Further, it is assumed that asphaltic concrete behaves as a linear system. Although it has been recognized that the behavior of this material is nonlinear particularly at higher stress levels and at higher temperatures, the investigations of Busching, Goetz and Harr (42) and others (43, 44) have established the validity of this assumption for small displacements normally encountered in bituminous mixtures.

RELATED THEORY

It has been pointed out in the previous section that asphaltic concrete can be considered as a continuous mechanical system in order to analyze its time-dependent response to an applied load and that transfer functions can be used to characterize this response. The basic theory behind the transfer functions is presented in this section.

Concept of Transfer Function

The ratio of an operational output (Laplace transform of the output) of a dynamical system to the operational input (Laplace transform of the input) is called the transfer function between the operational input and its corresponding output. The transfer function is shown schematically in Fig. 1. It is by definition a function of the complex variable s.

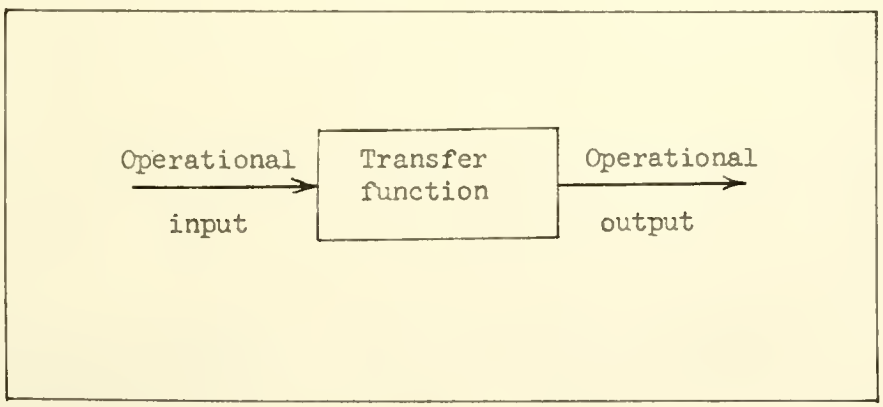

Fig. 1. Block diagram representation of the transfer function.

If a rigid body is subjected to a dynamical force f(t), then the force and the resulting displacement x(t) can be considered as the input and output respectively for the dynamical system. The transfer function between the operational force and the operational displacement is given by

$$G(s) = \frac{\bar{x}(s)}{\bar{f}(s)} \tag{10}$$

where $G(s)$ = the transfer function

$\bar{x}(s)$ = Laplace transform of the output

$\bar{f}(s)$ = Laplace transform of the input.

Solving for $\bar{x}(s)$,

$$\bar{x}(s) = G(s)\bar{f}(s) \tag{11}$$

The inverse transform of $\bar{x}(s)$ is x(t) and is

$$x(t) = \mathcal{L}^{-1}\{G(s)\bar{f}(s)\} \tag{12}$$

Eq. 12 shows that once the transfer function G(s) is known for any system, the displacement x(t) can be evaluated for that system for another given input force f(t).

In general, the transfer function G(s) is a ratio of two polynomials in s, such as

$$G(s) = \frac{N(s)}{D(s)} = \frac{(s - a_1')(s - a_2') \ldots (s - a_n')}{(s - b_1')(s - b_2') \ldots (s - b_m')} \tag{13}$$

where a_i' 's and b_i' 's are the roots or zeros of the numerator N(s) and denominator D(s) of G(s) respectively. b_i' 's are also called the poles

of G(s), since the transfer function becomes infinite when evaluated at a zero of its denominator. That is,

$$\lim_{s \to b_i'} G(s) \to \infty \tag{14}$$

Substituting for G(s) in Eq. 11, $\bar{x}(s)$ can be rewritten

$$\bar{x}(s) = \frac{\bar{f}(s)(s - a_1')(s - a_2')\ldots(s - a_n')}{(s - b_1')(s - b_2')\ldots(s - b_m')} \tag{15}$$

Eq. 15 can be expanded in m partial fractions for the m roots of D(s) as

$$\bar{x}(s) = \frac{C_1'}{(s - b_1')} + \frac{C_2'}{(s - b_2')} + \ldots. + \frac{C_m'}{(s - b_m')} \tag{16}$$

which is an identity in s where C_1', C_2', ..., C_m' are constants independent of s. Using the Laplace inverse transform, the final solution for x(t) is obtained from Eq. 16 (41) as

$$x(t) = C_1' e^{b_1' t} + C_2' e^{b_2' t} + \ldots + C_m' e^{b_m' t} \tag{17}$$

From the above discussion it is obvious that once the transfer function for a system is known, the displacement x(t) of the system for a given force input f(t) can be evaluated theoretically. The solutions for displacements for two specific cases of interest, namely, a sinusoidal load input and a step function input, are presented below for a system whose transfer function is given by G(s).

Solution for a Sinusoidal Input

Let the force input for the system whose transfer function is given by G(s) be

$$f(t) = f_o \sin \omega t, \tag{18}$$

where f_o is the magnitude of the sine function and ω is the time frequency. The operational displacement $\bar{x}(s)$ of the system is given by Eq. 11,

$$\bar{x}(s) = G(s)\bar{f}(s) \tag{11}$$

where

$$\begin{aligned}\bar{f}(s) &= \mathcal{L}\{f(t)\} \\ &= \mathcal{L}\{f_o \sin \omega t\} \\ &= \frac{f_o \omega}{s^2 + \omega^2} \end{aligned} \tag{19}$$

Substituting Eq. 19 in Eq. 11 and solving for x(t) by using the method of partial fractions,

$$\begin{aligned} x(t) &= \mathcal{L}^{-1}\{\bar{x}(s)\} \\ &= \mathcal{L}^{-1}\left\{\frac{G(s)\, f_o \omega}{s^2 + \omega^2}\right\} \\ &= f_o |G(j\omega)| \sin(\omega t + \phi), \end{aligned} \tag{20}$$

where ϕ is the phase angle between the input and the output, and t represents time.

Solution for a Step Function Input

A step function input is defined as

$$f(t) = 0 \qquad \text{for} \quad t < 0$$

$$f(t) = f_o \qquad \text{for} \quad t \geq 0 \tag{21}$$

where f_o is a constant with time as shown in Fig. 2. In view of this definition, for large times, a static compressive force of magnitude f_o applied to a system can be considered as a step function input.

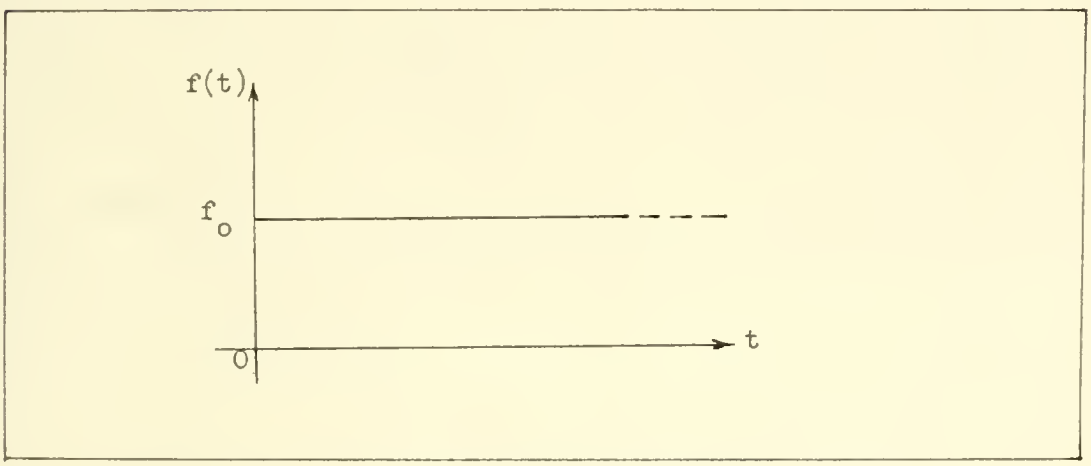

Fig. 2. A step function of time.

The Laplace transform of the step function f(t) is given by

$$\bar{f}(s) = \mathcal{L}\{f(t)\}$$

$$= \frac{f_o}{s} \tag{22}$$

As cited previously, the operational displacement of a system subjected to any force input is given by Eq. 11,

$$\bar{x}(s) = G(s)\bar{f}(s) \tag{11}$$

Substituting Eq. 22 into Eq. 11,

$$\bar{x}(s) = G(s)\frac{f_o}{s} \tag{23}$$

The inverse transform of $\bar{x}(s)$ is $x(t)$ which is obtained from

$$x(t) = \mathcal{L}^{-1}\left\{\frac{f_o G(s)}{s}\right\} \tag{24}$$

Assuming $G(s)$ of form

$$G(s) = \frac{A(s - a_1)(s - a_2)(s - a_3)}{(s - b_1)(s - b_2)(s - b_3)(s - b_4)} \tag{25}$$

as is the case in the present investigation, where A is a constant, a_i 's and b_i 's are zeros of the numerator and denominator respectively, $x(t)$ is obtained from Eq. 24, as

$$x(t) = \mathcal{L}^{-1}\left\{\frac{A\, f_o(s - a_1)(s - a_2)(s - a_3)}{(s - b_1)(s - b_2)(s - b_3)(s - b_4)s}\right\} \tag{26}$$

Eq. 26 can be solved using the method of partial fractions which yields

$$x(t) = C_1 e^{b_1 t} + C_2 e^{b_2 t} + C_3 e^{b_3 t} + C_4 e^{b_4 t} + C_5 \tag{27}$$

where C_i 's are constants independent of t.

Determination of the Transfer Function

The experimental basis to obtain the transfer function is the frequency spectrum. A sinusoidal input of known magnitude and frequency is

applied to the system whose transfer function is sought. The magnitude of the steady-state output and the phase angle between the output and the input are then measured. It is necessary to make certain that the output is only the steady-state component (after the transient component has been assumed to have damped out) by measuring its frequency and ascertaining that it is the same as that of the input. In a frequency spectrum analysis, interest is in the ratio of magnitude and not in the value of each of the magnitudes of the input and steady-state output.

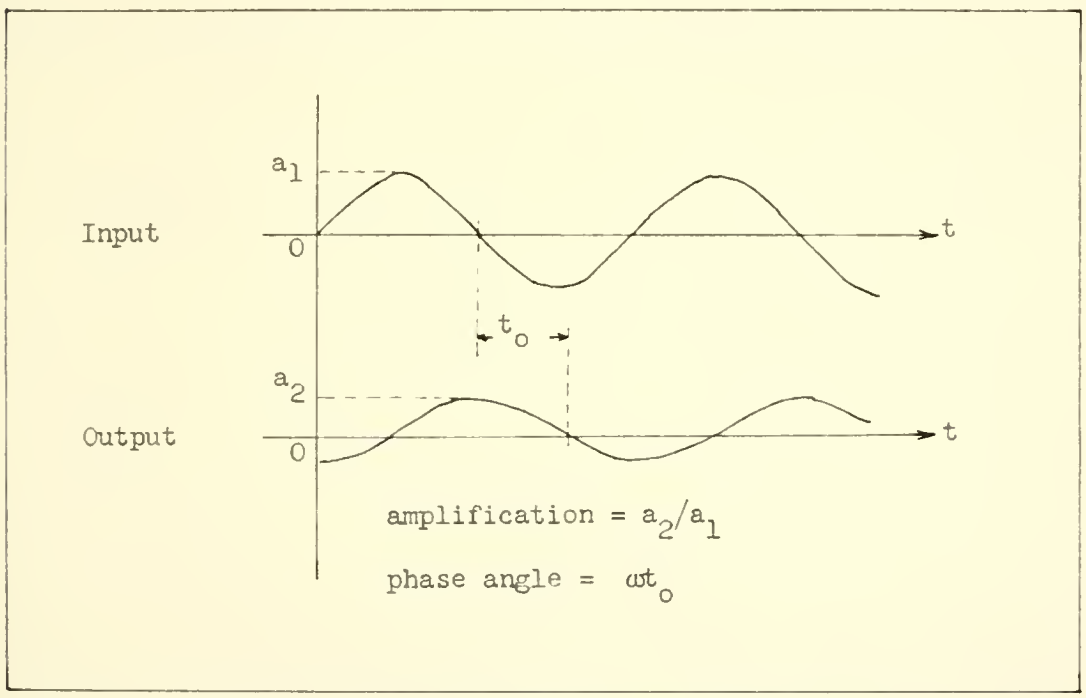

Fig. 3. Experimental magnitude and phase measurements.

The ratio of the magnitude of the output to that of the input is called the amplification or gain. The amplification and phase angle are therefore experimentally determined at a given frequency. The frequency of the input is then changed to another value and again the amplification

and phase angle are determined. The procedure continues from a very low frequency (approximately zero) to that frequency at which the output magnitude is approximately zero. The plot of the amplification against frequency is called the frequency spectrum, and for convenience the magnitude of the amplification is plotted in decibels*. Fig. 3 shows the input and output traces for a given frequency.

Once the amplification is plotted against log of frequency, the curve may be approximated with a series of connected straight lines as shown in Fig. 4. These straight lines are selected so as to form asymptotes to the curve. Although straight lines of any slope may be used, the slopes of

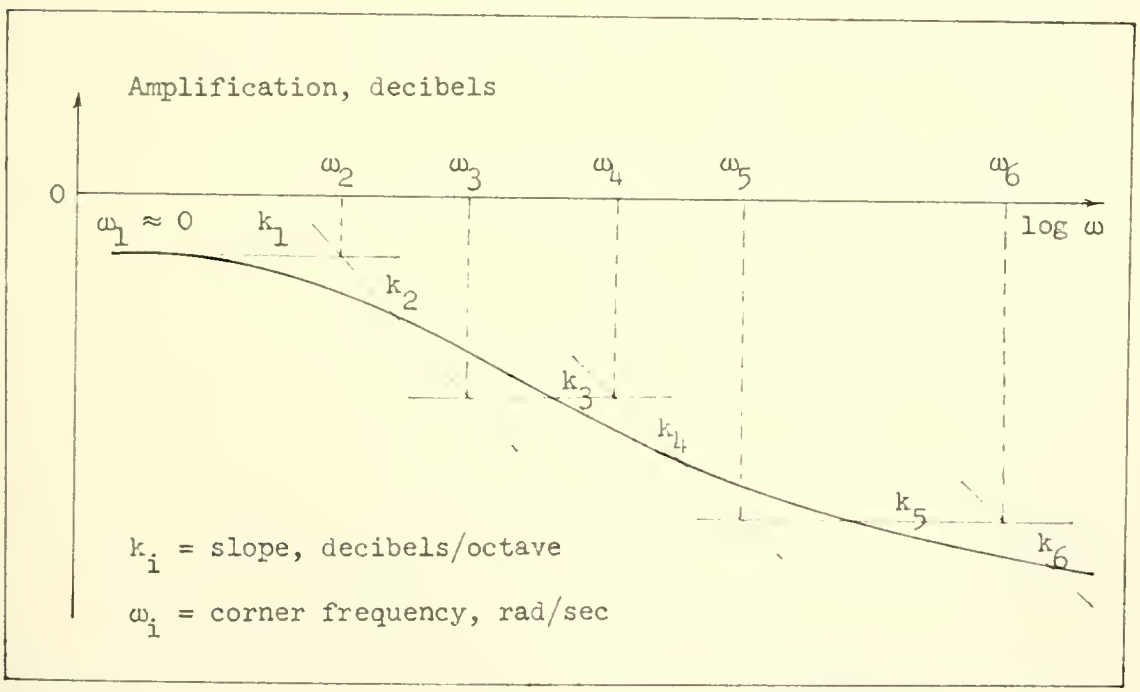

Fig. 4. Asymptotic approximation of a frequency spectrum.

---

* $R_{db} = 20 \log_{10} R$

the asymptotes are generally taken to be six decibels per octave* for greater ease of determination. The closer the approximation to the actual frequency spectrum curve, the better will be the approximation of the transfer function being sought (41).

The intersections of the selected approximating asymptotes determine the corner frequencies. In Fig. 4 these are six: $\omega_1 = 0$, ω_2, ω_3, ω_4, ω_5 and ω_6. The slopes of the asymptotes are given by k_1, k_2, k_3, k_4, k_5 and k_6 decibels per octave. Once the corner frequencies and the slopes of the approximating asymptotes are obtained, the modified transfer function which describes the frequency spectrum is written (41) as

$$G(j\omega) \cong A(j\omega + \omega_1)^{\frac{k_1}{6}} (j\omega + \omega_2)^{\frac{k_2-k_1}{6}} (j\omega + \omega_3)^{\frac{k_3-k_2}{6}} \ldots (j\omega + \omega_n)^{\frac{k_n-k_{n-1}}{6}} \quad (28)$$

The modified transfer function is the vector amplification or simply the ratio of the magnitude of the output to that of the input and is a function of the input frequency. By substituting $s = j\omega$ in Eq. 28, the transfer function for the system is obtained

$$G(s) \cong A(s + \omega_1)^{\frac{k_1}{6}} (s + \omega_2)^{\frac{k_2-k_1}{6}} (s + \omega_3)^{\frac{k_3-k_2}{6}} \ldots (s + \omega_n)^{\frac{k_n-k_{n-1}}{6}} \quad (29)$$

The constant A can be determined from any one experimental frequency in the frequency spectrum by calculating the absolute value of the transfer function from Eq. 28 at that frequency and equating it to the corresponding amplification value in the frequency spectrum.

---

* An octave is defined as the frequency range for which the ratio of the upper bound frequency to the lower bound frequency is 2 to 1; that is, $\omega_i < \omega < 2\omega_i$ is an octave.

A typical example of determining the transfer function and the constant A from a frequency spectrum obtained for a bituminous concrete specimen is given in the Appendix.

It must be noted that this method of obtaining the approximate transfer function from the frequency spectrum is applicable only for an overdamped or critically damped system. It may be used in the present investigation because bituminous mixes have been observed to behave as overdamped systems.

EXPERIMENTAL INVESTIGATION

The experimental phase of this study had as an objective the development and use of accurate techniques for obtaining all of the data required in the determination of the transfer function from a frequency spectrum. The core of the technique lies in devising a system which can apply a sinusoidal force input of a desired magnitude and frequency and which can simultaneously measure the displacement output.

An MTS electronic function generator coupled with a loading frame which was fitted with an electronically controlled hydraulic actuator was used for this purpose. See Figs. 5 and 6. The loading frame was installed in a constant temperature room which facilitated carrying out the tests at the desired temperatures. A two-channel Brush recorder which was attached to the function generator recorded the input and output of the test specimen simultaneously.

Dynamic Tests

The function generator was used to apply sinusoidal force inputs to the asphaltic concrete specimen by suitable manipulation of the controls. The magnitudes of the sine force varied from 2.5 to 15 lbs. and the frequencies varied from 0.0016 to 1.6 cycles per second.

Since in a sine test the specimen is alternatively in compression and in tension, the method of mounting the specimen in the test assembly was of paramount importance. Two aluminum plates, 2 in. x 2 in. x 3/8 in. in size, were glued to the specimen top and bottom respectively, using

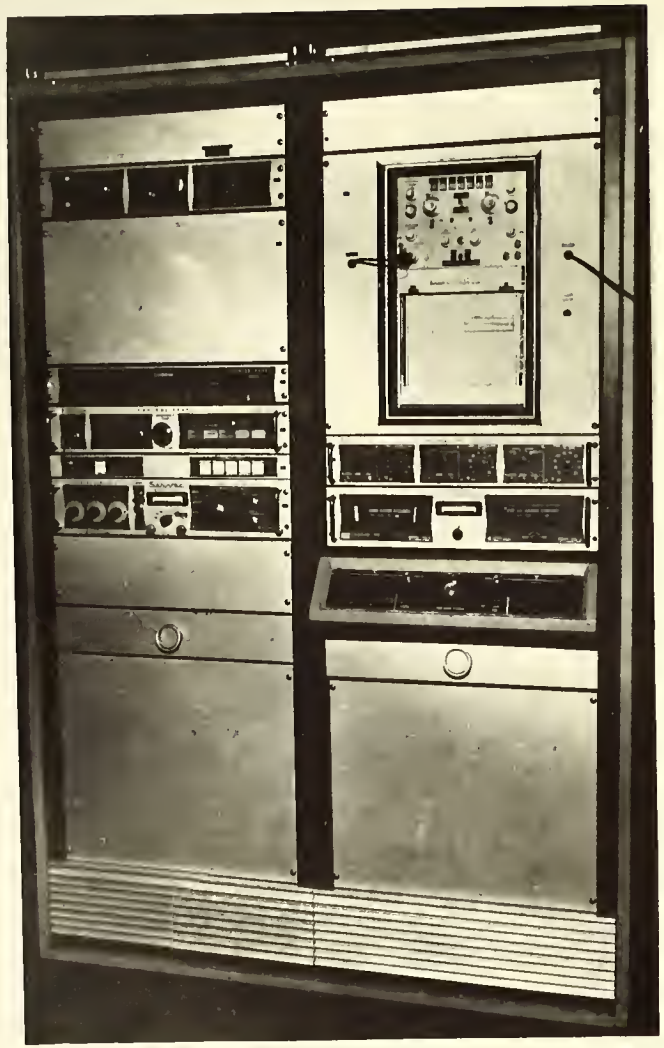

Fig. 5. Function Generator

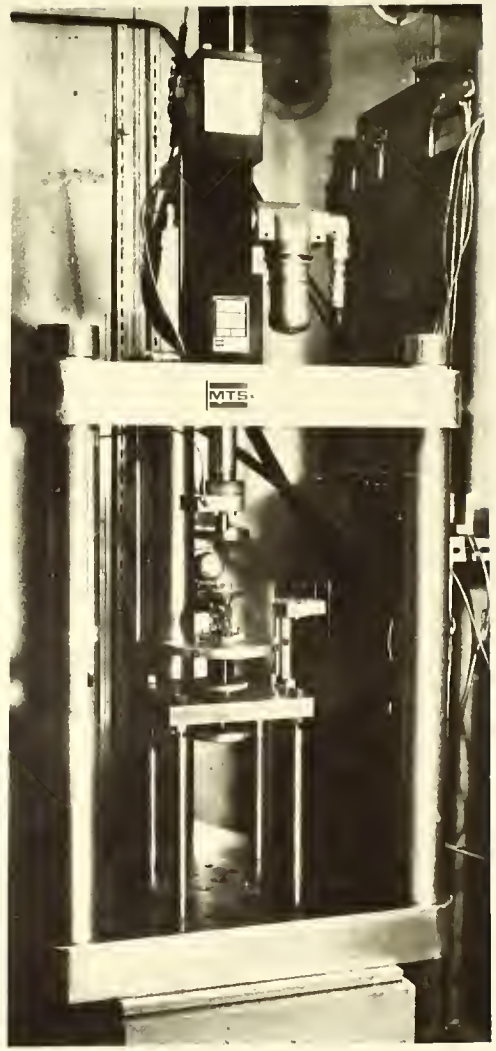

Fig. 6. Loading Frame

commercially available Eastman 910 Adhesive. See Fig. 7. The plates, in turn, were connected to the top and bottom loading platens by screws and nuts. The top platen was rigidly fixed to the moving ram of the hydraulic actuator while the bottom platen was fixed to the loading deck. See Fig. 8. Remotely controlled and commanded by the electronic console of the function generator, the hydraulic ram moves up and down at the pre-set sine force and frequency. Thus the specimen was subjected to the desired sinusoidal force input which was recorded by the left channel of the Brush recorder. The corresponding displacement of the specimen was sensed by the LVDT in the actuator and was simultaneously recorded as the output in the right channel of the recorder. Fig. 9 shows the two traces thus obtained in a typical dynamic test.

Static Tests

The same test assembly which was used for the dynamic tests was used for the static tests. When the function generator is set for a combination of a ramp function and a high frequency, the actuator applies a static compressive force of desired magnitude. As before, the left and right channels recorded the input and output respectively. The two traces of a typical static compression test are illustrated in Fig. 10.

Materials and Preparation of Specimens

Two different gradings, one with a maximum size of the No. 4 sieve and the other the 3/8 inch sieve were used in this investigation. The bituminous mixes prepared on the basis of these gradings were designated as Mix-1 and Mix-2, respectively. Table 1 shows the sieve analysis and origin of the aggregates used. The grading curves are given in Fig. 11.

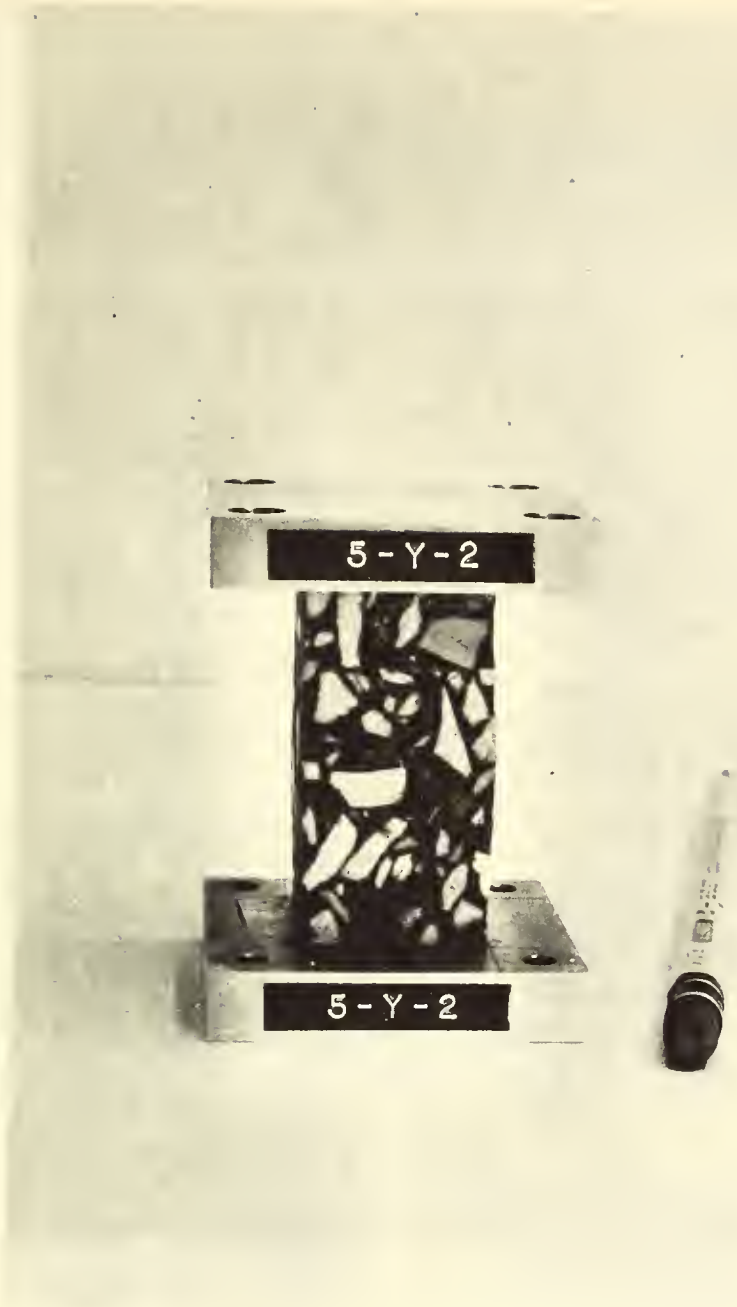

Fig. 7. A Typical Test Specimen

Fig. 8. Specimen in Position for Testing

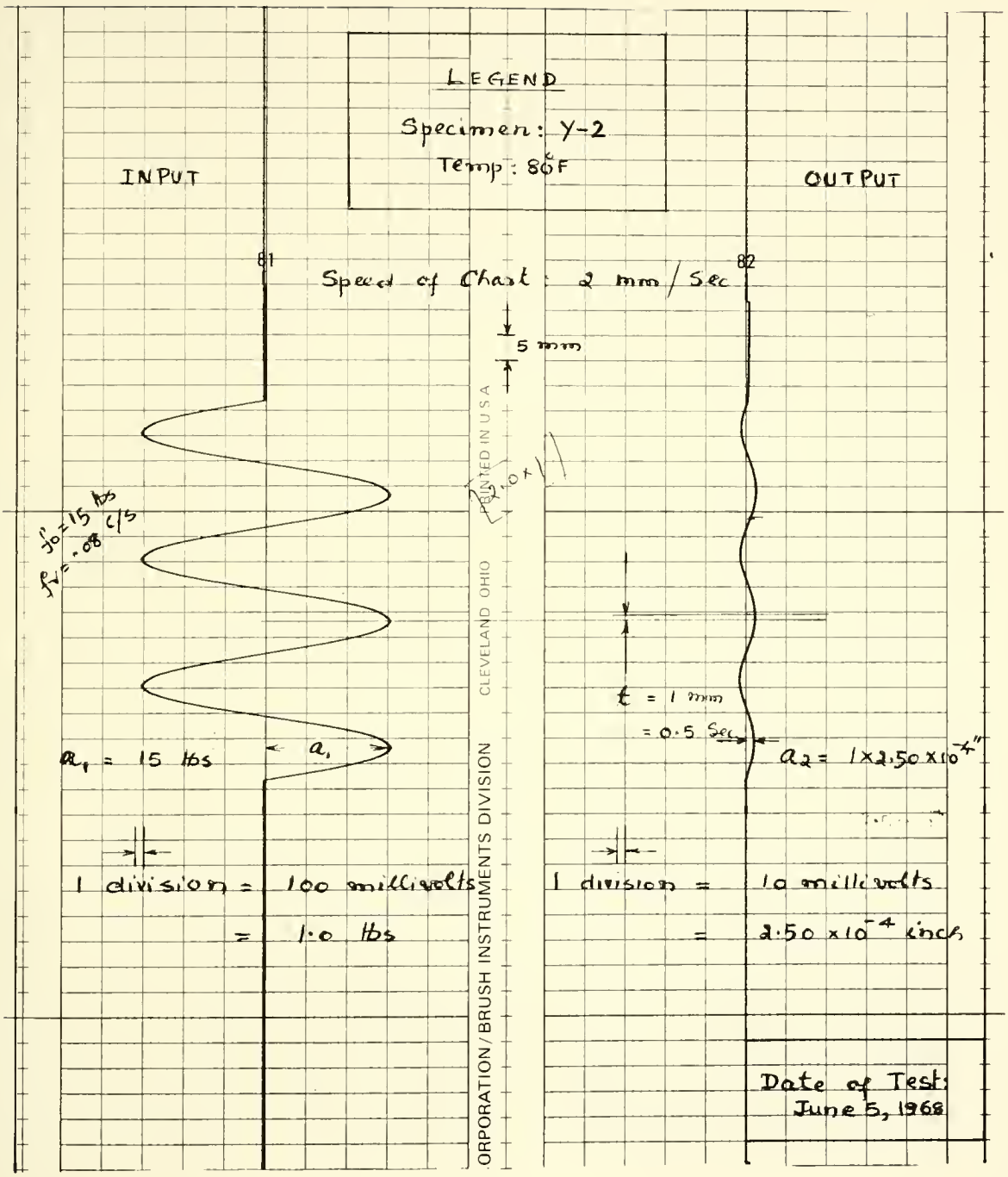

Fig. 9. Typical traces of a sinusoidal loading test.

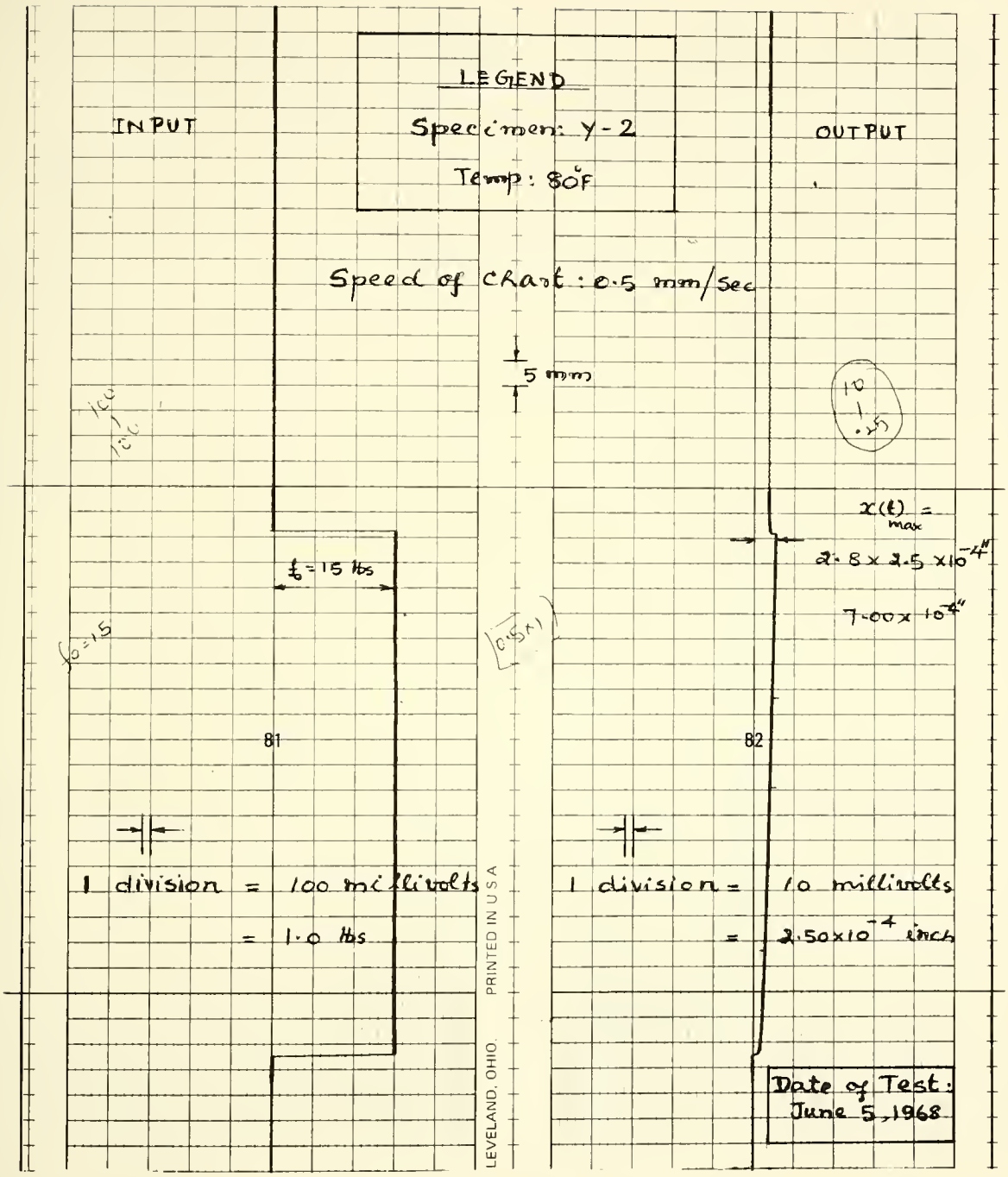

Fig. 10. Typical traces of a static compression test.

TABLE 1

Sieve Analysis of Aggregates

Sieve		Fraction, %		Material
Passing	Retained	Mix-1	Mix-2	
3/8 in.	No. 4	...	35	Crushed Limestone
No. 4	No. 6	17	11	" "
No. 6	No. 8	13	11	" "
No. 8	No. 16	20	18	River Sand
No. 16	No. 30	17	10	" "
No. 30	No. 50	13	7	" "
No. 50	No. 100	10	4	" "
No. 100	No. 200	5	2	" "
No. 200		5	2	Limestone Filler

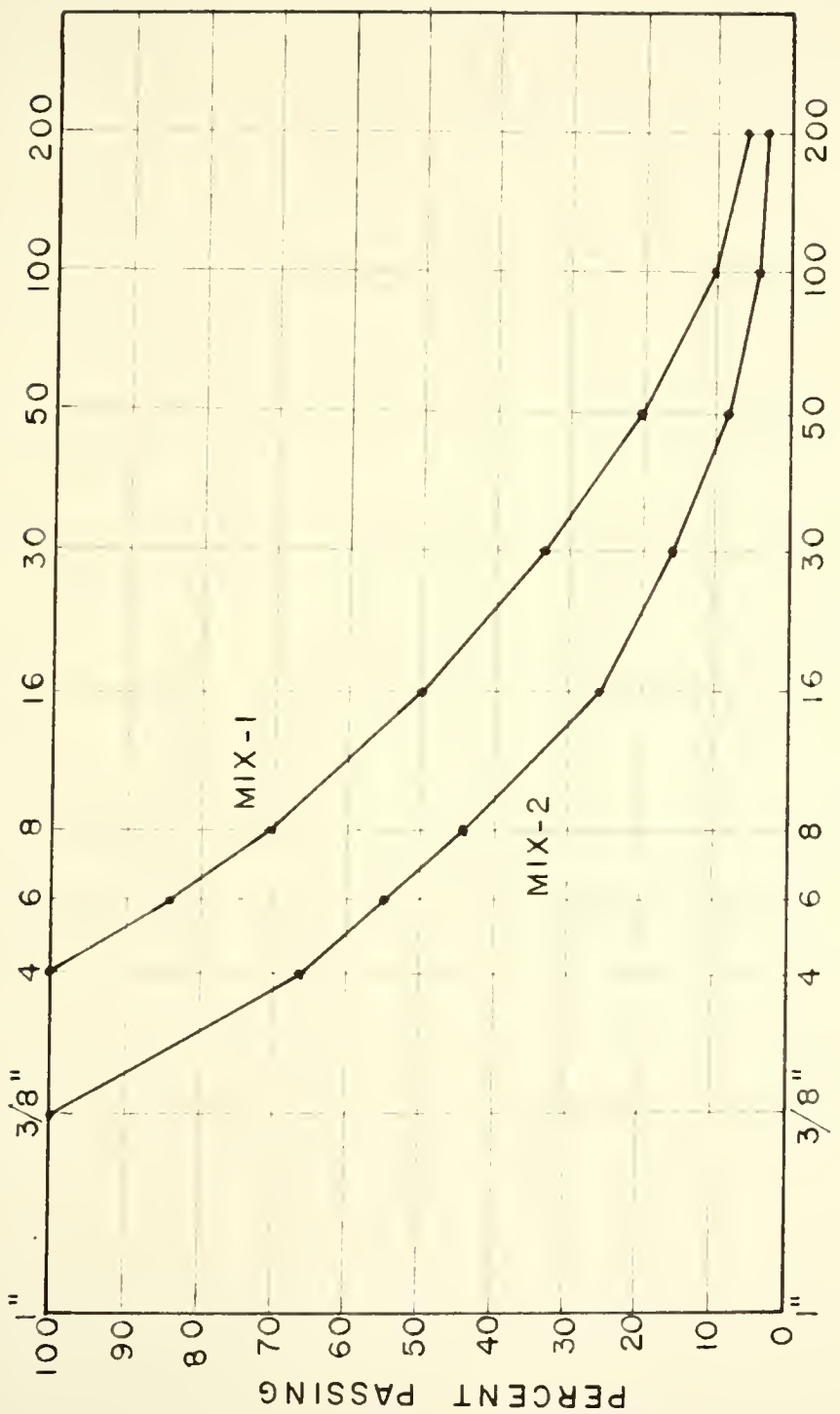

Fig. 11. Grading curves for Mix-1 and Mix-2

A 60-70 penetration asphalt cement having the properties shown in Table 2 was used. After being blended in 2200 gram batches, the aggregate was placed in an oven and heated to 325°F. The asphalt was heated to 325°F and then mixed with the heated aggregate in a mechanical mixer for two minutes. The weight of asphalt cement mixed with the aggregate was 5.0 and 3.5 percent by weight of the aggregate for Mix-1 and Mix-2, respectively. After mixing was completed, each batch was put in flat pans and placed in a forced-draft oven to cure for 24 hours at 140°F.

Compaction of the bituminous mixture was started after the mixture was reheated to 325°F. The heated mixture was placed in two layers in the heated beam mold of internal dimensions 2 in. x 2 1/2 in. x 12 in. Each layer was rodded 25 times with a 1/2-inch diameter, round-end tamping rod. The mixture in the beam mold was compacted with the kneading compactor by the use of a special rectangular tamping foot of size 2 in. x 2 1/2 in. The mixture was compacted with the tamping foot by moving the mold back and forth its entire length under the tamping foot four times, using eight tamps during each one-way traverse for each of four different compaction pressures. Foot pressures used in compaction were 20, 35, 100 and 120 psi in that order. After the beam was compacted on its top side according to this procedure, the mold and beam were inverted and the procedure was repeated. Hence, both the top and the bottom of the beam received the same compactive effort.

After the beam was compacted, it was removed from the mold and placed in a forced-draft oven and cured for 24 hours at a temperature of 140°F. After the curing period, the beam was cooled to room temperature.

The compacted beam was cut into specimens by use of a masonry saw.

TABLE 2

Results of Tests on Asphalt Cement

Specific Gravity at 77°F	1.036
Softening Point, Ring and Ball, °F	124
Ductility at 77°F, 5 cm/min, cm	100+
Penetration, 100 grams, 5 sec., 77°F	63
Penetration, 200 grams, 60 sec., 32°F	17
Loss on Heating, 50 grams, 5hr., 325°F, %	0.01
Penetration of Residue, % of Original	89
Flash Point, Cleveland Open Cup, °F	595
Solubility in CCl_4, %	99.84

One-inch pieces were cut from both ends of the beams and wasted. This was done because it was recognized that confinement at the ends of the beam mold might cause compaction conditions to be atypical at these locations. Specimens were cut along the x, y, and z axes of the beam, as shown in Fig. 12, approximately 0.05 inch oversize. Final shaping and polishing were accomplished on a lapping wheel using 100 and 800 mesh grinding compounds successively. The dimensions of the test specimens were controlled to 0.01 inch by utilizing the jig shown in Fig. 13, and the final dimensions were 1 in. x 1 in. x 2 in.

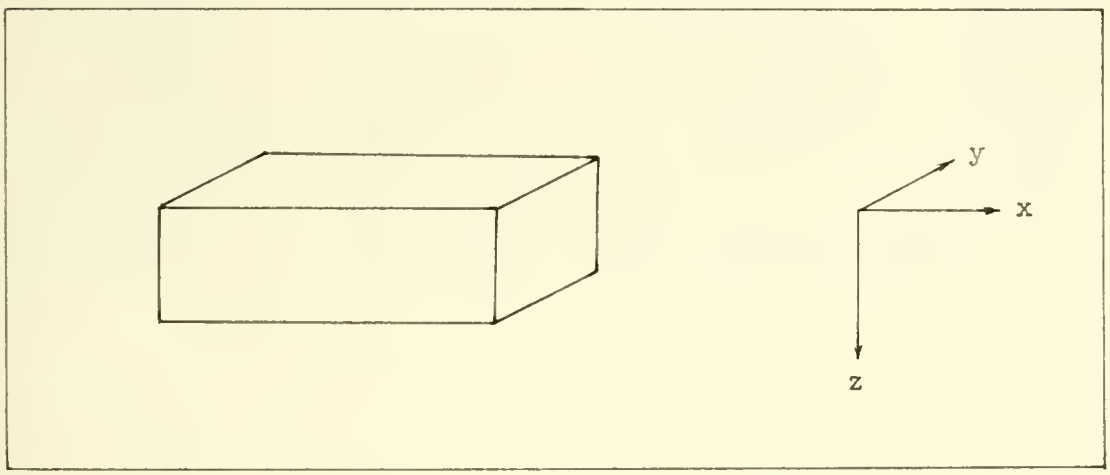

Fig. 12. Designation of axes for the beam.

Scope

The investigation was confined to the two bituminous mixes described in the previous section and to three temperatures, namely, 70, 80 and 90°F. For each mix three different specimens cut along the x, y and z directions of the beam were used. The specimens were designated as x-1, y-1, z-1, x-2, y-2 and z-2, the letter denoting the axis along which it was cut and

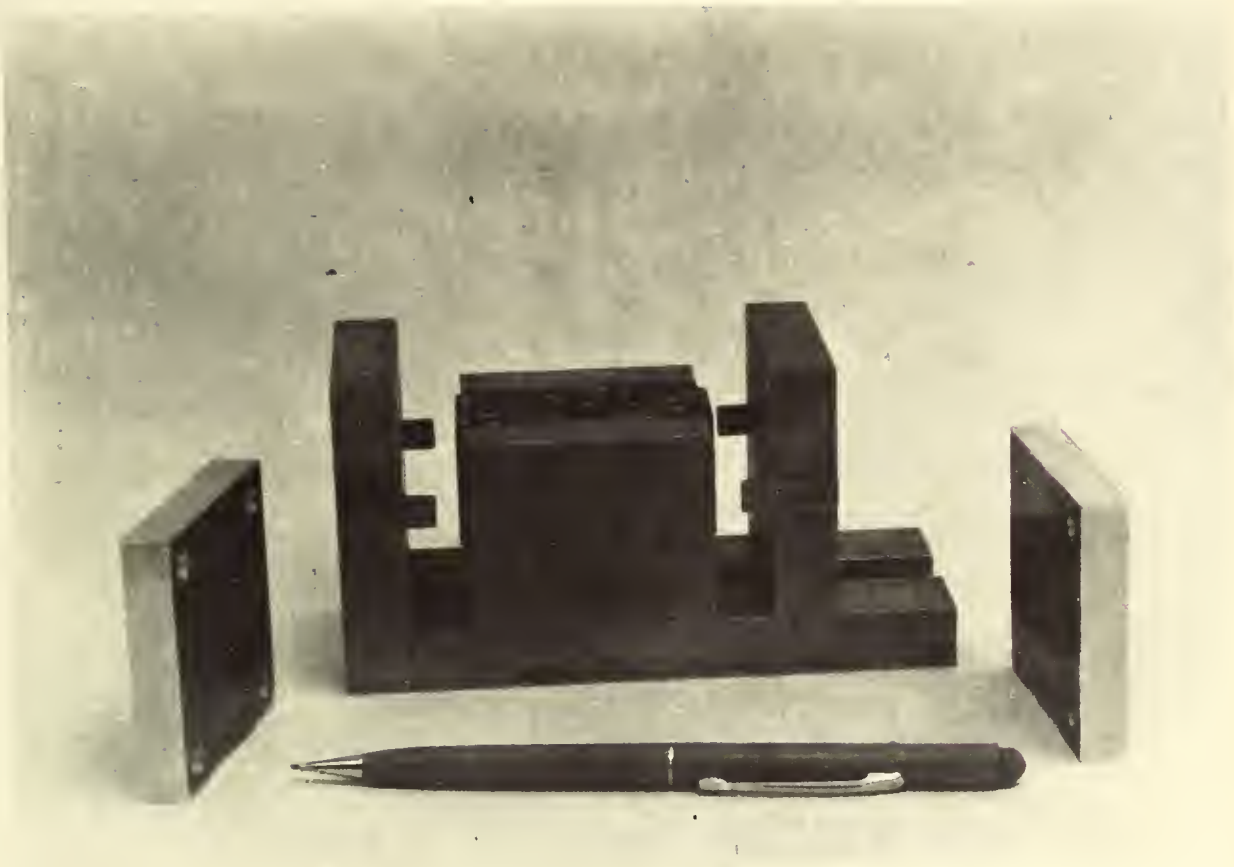

Fig. 13. Jig for Specimen Alignment

the numeral the mix.

In order to investigate the effect of size of specimen on the transfer function, three different-sized specimens from Mix-1 were tested at one temperature, namely, 90°F. Keeping the height-width ratio constant, the following three sizes were used: 3/4 in. x 3/4 in. x 1 1/2 in., 1 in. x 1 in. x 2 in. and 1 1/4 in. x 1 1/4 in. x 2 1/2 in.

RESULTS OF EXPERIMENTS

The results of all the dynamic and static tests at 70, 80 and 90°F are summarized in Tables 3 through 10. The transfer functions derived for each specimen at these temperatures are shown in Tables 3, 4 and 5. The calculated displacements for each specimen for three different sinusoidal load inputs and constant load inputs, respectively, and the corresponding measured displacements are shown in Tables 6, 7 and 8.

The phase angles obtained in the dynamic tests for each specimen are shown separately in Table 9 with respect to the frequency of the test. The same data are shown graphically in Figs. 14 through 19.

The absolute value of G(s) versus frequency curves for the six specimens from the two different mixes tested at the three different temperatures are shown in Fig. 22.

TABLE 3

Transfer Functions at 70°F

Specimen	Transfer Function
z-1	$G(s) = \frac{(0.035)(s + 0.031)(s + 0.18)(s + 1.7)}{(s + 0.02)(s + 0.1)(s + 1)(s + 10)}$
x-1	$G(s) = \frac{(0.0242)(s + 0.02)(s + 0.18)(s + 1.6)}{(s + 0.014)(s + 0.1)(s + 1)(s + 10)}$
y-1	$G(s) = \frac{(0.0348)(s + 0.03)(s + 0.4)(s + 2.7)}{(s + 0.02)(s + 0.25)(s + 2)(s + 10)}$
z-2	$G(s) = \frac{(0.032)(s + 0.025)(s + 0.16)(s + 1.8)}{(s + 0.02)(s + 0.1)(s + 1)(s + 10)}$
x-2	$G(s) = \frac{(0.0356)(s + 0.025)(s + 0.16)(s + 1.6)}{(s + 0.02)(s + 0.1)(s + 1)(s + 10)}$
y-2	$G(s) = \frac{(0.0356)(s + 0.025)(s + 0.16)(s + 1.6)}{(s + 0.02)(s + 0.1)(s + 1)(s + 10)}$

TABLE 4

Transfer Functions at 80°F

Specimen	Transfer Function
z-1	$G(s) = \frac{(0.05)(s + 0.025)(s + 0.2)(s + 2)}{(s + 0.02)(s + 0.1)(s + 1)(s + 10)}$
x-1	$G(s) = \frac{(0.0415)(s + 0.028)(s + 0.17)(s + 1.8)}{(s + 0.02)(s + 0.1)(s + 1)(s + 10)}$
y-1	$G(s) = \frac{(0.04)(s + 0.025)(s + 0.16)(s + 2.3)}{(s + 0.02)(s + 0.1)(s + 1)(s + 10)}$
z-2	$G(s) = \frac{(0.04)(s + 0.025)(s + 0.16)(s + 2.3)}{(s + 0.02)(s + 0.1)(s + 1)(s + 10)}$
x-2	$G(s) = \frac{(0.0415)(s + 0.028)(s + 0.17)(s + 1.8)}{(s + 0.02)(s + 0.1)(s + 1)(s + 10)}$
y-2	$G(s) = \frac{(0.0415)(s + 0.028)(s + 0.17)(s + 1.8)}{(s + 0.02)(s + 0.1)(s + 1)(s + 10)}$

TABLE 5

Transfer Functions at 90°F

Specimen	Transfer Function
z-1	$G(s) = \frac{(0.1)(s + 0.02)(s + 0.2)(s + 1.7)}{(s + 0.015)(s + 0.1)(s + 1)(s + 10)}$
x-1	$G(s) = \frac{(0.082)(s + 0.03)(s + 0.2)(s + 1.6)}{(s + 0.02)(s + 0.1)(s + 1)(s + 10)}$
y-1	$G(s) = \frac{(0.1)(s + 0.02)(s + 0.17)(s + 2.0)}{(s + 0.015)(s + 0.1)(s + 1)(s + 10)}$
z-2	$G(s) = \frac{(0.07)(s + 0.03)(s + 0.17)(s + 2.5)}{(s + 0.02)(s + 0.1)(s + 1)(s + 10)}$
x-2	$G(s) = \frac{(0.085)(s + 0.02)(s + 0.2)(s + 1.8)}{(s + 0.015)(s + 0.1)(s + 1)(s + 10)}$
y-2	$G(s) = \frac{(0.085)(s + 0.02)(s + 0.2)(s + 1.8)}{(s + 0.015)(s + 0.1)(s + 1)(s + 10)}$

TABLE 6

Calculated and Measured Displacements at 70°F

Specimen	Sine Load Input				Constant Load Input		
	f_o	ω	$\hat{x}(t)$		f_o	$\hat{x}(t)$	
			calculated	measured		calculated	measured
	lbs	rad/sec	inch($\times 10^{-4}$)	inch($\times 10^{-4}$)	lbs	inch($\times 10^{-4}$)	inch($\times 10^{-4}$)
z-1	5	0.025	1.63	1.75	5	2.08	1.75
	5	2.500	0.44	0.50	10	4.16	2.50
	5	5.000	0.38	0.38	20	8.32	5.50
x-1	5	2.500	0.48	0.50	10	2.75	2.50
	15	0.025	3.20	3.25	20	5.50	5.00
	15	0.100	2.25	2.25	30	8.25	6.25
y-1	15	0.025	3.52	3.00	10	2.80	2.50
	15	0.016	2.63	2.25	20	5.60	4.50
	15	0.250	2.25	2.00	30	8.40	7.00
z-2	15	0.025	3.75	3.75	10	2.90	2.75
	15	0.100	2.90	3.00	20	5.80	5.00
	15	0.250	2.33	2.35	30	8.70	8.25
x-2	15	0.025	3.75	3.75	10	2.85	2.75
	15	0.100	2.85	2.75	20	5.70	5.00
	15	0.250	2.33	2.25	30	8.55	8.00
y-2	15	0.025	3.75	3.50	10	2.85	2.75
	15	0.100	2.85	2.50	20	5.70	5.75
	15	0.250	2.33	2.00	30	8.55	9.25

TABLE 7

Calculated and Measured Displacements at 80°F

Specimen	Sine Load Input				Constant Load Input		
	f_o	ω	$x(t)$		f_o	$x(t)$	
			calculated	measured		calculated	measured
	lbs	rad/sec	inch ($x10^{-4}$)	inch($x10^{-4}$)	lbs	inch($x10^{-4}$)	inch($x10^{-4}$)
z-1	5	0.05	2.37	2.25	5	3.13	2.50
	5	0.50	1.20	1.25	10	6.26	5.00
	5	5.00	0.58	0.50	15	9.39	10.00
x-1	5	0.05	1.59	1.25	5	2.23	2.00
	5	0.50	0.87	0.75	10	4.46	3.75
	5	5.00	0.50	0.50	15	6.69	5.50
y-1	15	0.05	5.32	5.00	5	2.30	2.25
	15	0.50	3.18	3.00	10	4.60	4.00
	15	5.00	1.43	1.75	15	6.90	8.75
z-2	15	0.05	5.32	5.00	5	2.30	2.25
	15	0.50	3.18	3.00	10	4.60	4.50
	15	5.00	1.43	1.50	15	6.90	6.50
x-2	15	0.05	4.76	5.00	5	2.23	1.25
	15	0.50	2.62	2.50	10	4.46	4.00
	15	5.00	1.50	1.75	15	6.69	9.50
y-2	15	0.05	4.76	4.75	5	2.23	2.25
	15	0.50	2.62	2.50	10	4.46	4.00
	15	5.00	1.50	1.50	15	6.69	7.00

TABLE 8

Calculated and Measured Displacements at 80°F

Specimen	Sine Load Input				Constant Load Input		
	f_o	ω	$x(t)$		f_o	$x(t)$	
			calculated	measured		calculated	measured
	lbs	rad/sec	inch($\times 10^{-4}$)	inch($\times 10^{-4}$)	lbs	inch($\times 10^{-4}$)	inch($\times 10^{-4}$)
z-1	5	0.05	4.00	3.75	5	5.65	4.50
	5	0.50	2.06	1.88	10	11.30	7.50
	5	5.00	1.12	1.00	15	16.95	16.30
x-1	5	0.05	3.25	2.75	5	5.00	2.50
	5	0.50	1.62	1.75	10	10.00	8.75
	5	5.00	0.87	0.87	15	15.00	11.20
y-1	5	0.05	4.00	4.00	5	5.65	5.00
	5	0.50	2.37	2.37	10	11.30	10.00
	5	5.00	1.25	1.25	15	16.95	15.00
z-2	5	0.05	3.75	3.75	2.5	2.78	2.75
	5	0.50	2.00	2.00	5	5.56	5.25
	5	5.00	0.87	0.75	10	11.12	13.00
x-2	10	0.50	3.75	3.75	2.5	2.56	2.00
	10	1.00	3.25	3.25	5	5.12	4.75
	10	5.00	2.00	2.25	10	10.24	9.50
y-2	10	0.50	3.75	4.25	2.5	2.56	2.00
	10	1.00	3.25	3.25	5	5.12	4.00
	10	5.00	2.00	2.25	10	10.24	9.50

TABLE 9

Phase Angles

Temp	Specimen	ϕ, deg. at ω, rad/sec								
°F		0.025	0.05	0.1	0.25	0.5	1.0	2.5	5.0	10.0
70	z-1	18.6	21.5	20.6	17.2	14.3	11.4	11.4	10.0	5.7
	x-1	14.4	14.4	11.5	10.4	8.6	6.9	5.7	5.7	-
	y-1	17.8	23.0	23.0	21.5	14.4	11.5	10.0	7.2	5.7
	z-2	18.3	21.5	23.0	18.6	14.4	11.5	11.5	7.3	5.7
	x-2	18.2	21.5	18.2	14.4	11.5	11.5	8.6	7.2	5.7
	y-2	18.2	21.5	18.2	18.2	11.5	9.2	7.2	7.2	5.7
80	z-1	21.8	23.9	23.8	21.5	19.5	17.8	15.5	13.2	12.0
	x-1	18.0	20.2	22.5	21.3	18.6	16.0	13.0	11.2	10.0
	y-1	32.2	33.4	29.8	28.7	28.7	24.1	21.5	20.1	17.3
	z-2	28.7	40.0	34.5	34.5	28.7	25.8	21.2	14.4	11.4
	x-2	28.7	28.7	34.5	28.7	22.2	25.2	14.4	14.4	11.4
	y-2	28.6	31.5	31.5	25.1	23.0	23.0	21.5	21.5	17.2
90	z-1	18.2	23.0	23.0	18.2	11.5	11.5	8.6	7.2	5.7
	x-1	18.2	25.8	23.0	17.2	14.4	11.5	8.6	7.2	5.7
	y-1	18.2	24.5	23.0	17.2	14.4	11.5	8.6	7.2	5.7
	z-2	21.5	23.0	23.0	17.2	14.4	11.5	9.7	7.2	5.7
	x-2	21.5	28.6	23.0	17.2	14.3	11.5	8.6	7.1	5.7
	y-2	21.5	25.8	23.0	15.5	17.2	11.5	11.5	7.2	5.7

TABLE 10

Results of a Typical Sinusoidal Test

Specimen: z-1

Test Temperature: 80°F

ω rad/sec	a_1 mv	a_2 mv	$R = \frac{a_2}{a_1}$	R_{db}	t sec	ϕ rad	ϕ deg.
0.025	1000	22.0	0.0220	-33.1520	15.30	0.382	21.8
0.050	"	19.5	0.0195	-34.4240	8.32	0.416	23.9
0.100	"	17.0	0.0170	-35.3920	4.15	0.415	23.8
0.250	"	11.0	0.0110	-39.1720	1.50	0.375	21.5
0.500	"	9.0	0.0090	-40.9160	0.68	0.340	19.5
1.000	"	8.0	0.0080	-41.9380	0.311	0.311	17.8
2.500	"	6.5	0.0065	-43.7420	0.110	0.271	15.5
5.000	"	5.0	0.0050	-46.0200	0.046	0.230	13.2
10.000	"	4.0	0.0040	-47.9580	0.021	0.210	12.0

LEGEND

ω = input frequency, rad/sec

a_1 = input magnitude, millivolts

a_2 = output magnitude, millivolts

$R = a_2/a_1$

R_{db} = R expressed in decibels

$= 20 \log_{10} R$

t = time lag between input and output, sec.

ϕ = phase lag between input and output

$= \omega t$ radians.

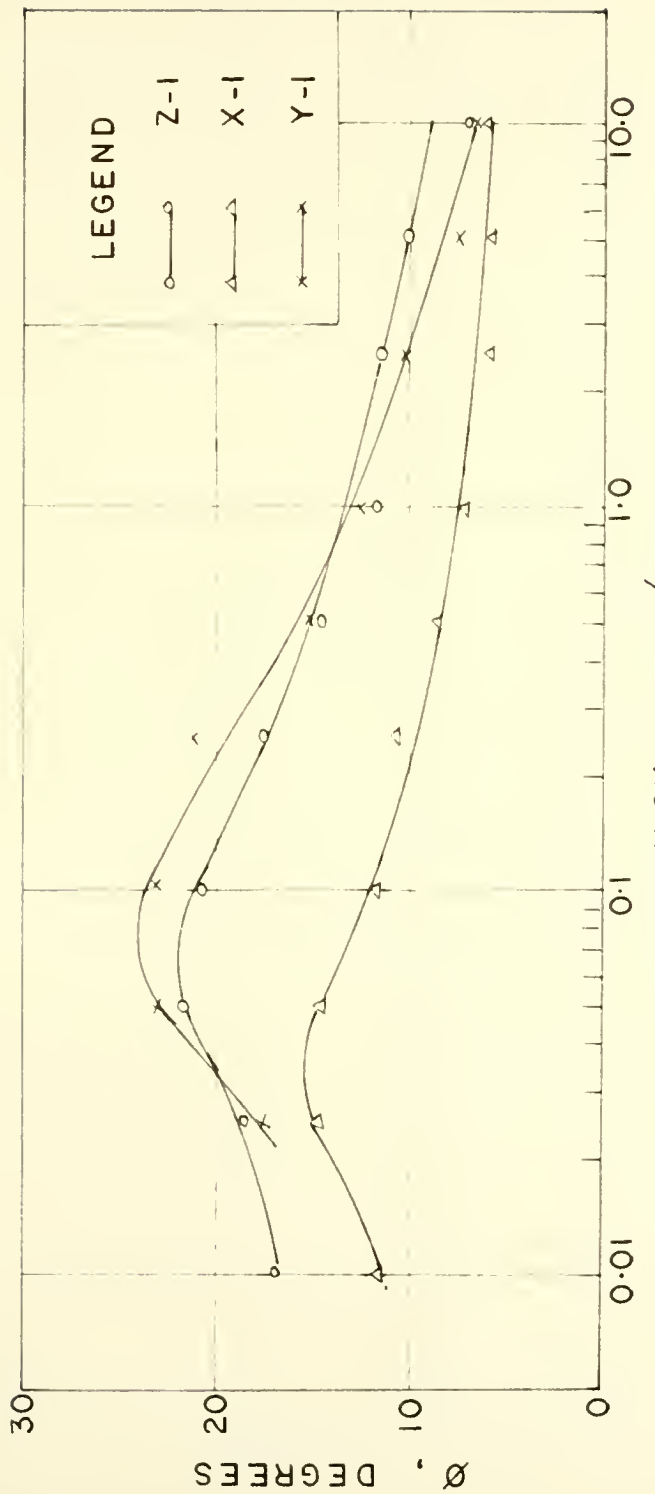

Fig. 14. Phase angle versus frequency for Mix-1 at 70°F

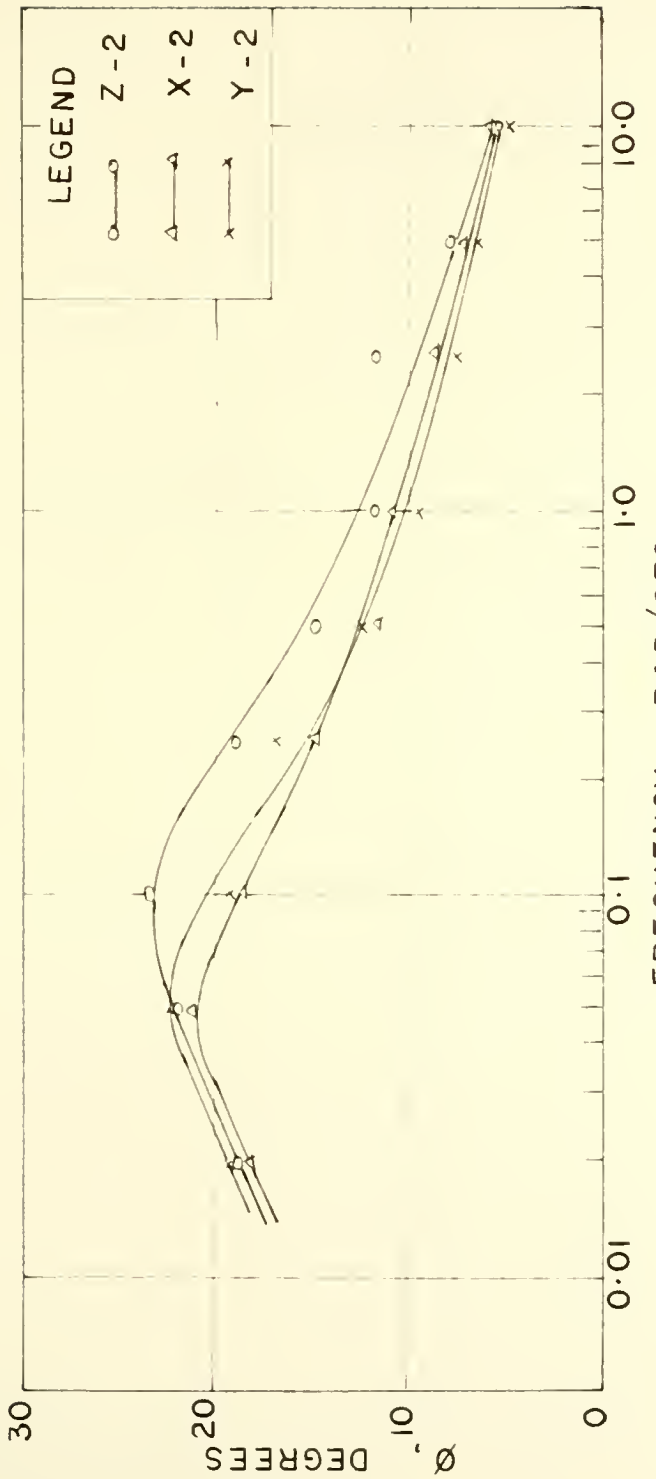

Fig. 15. Phase angle versus frequency for Mix-2 at 70°F

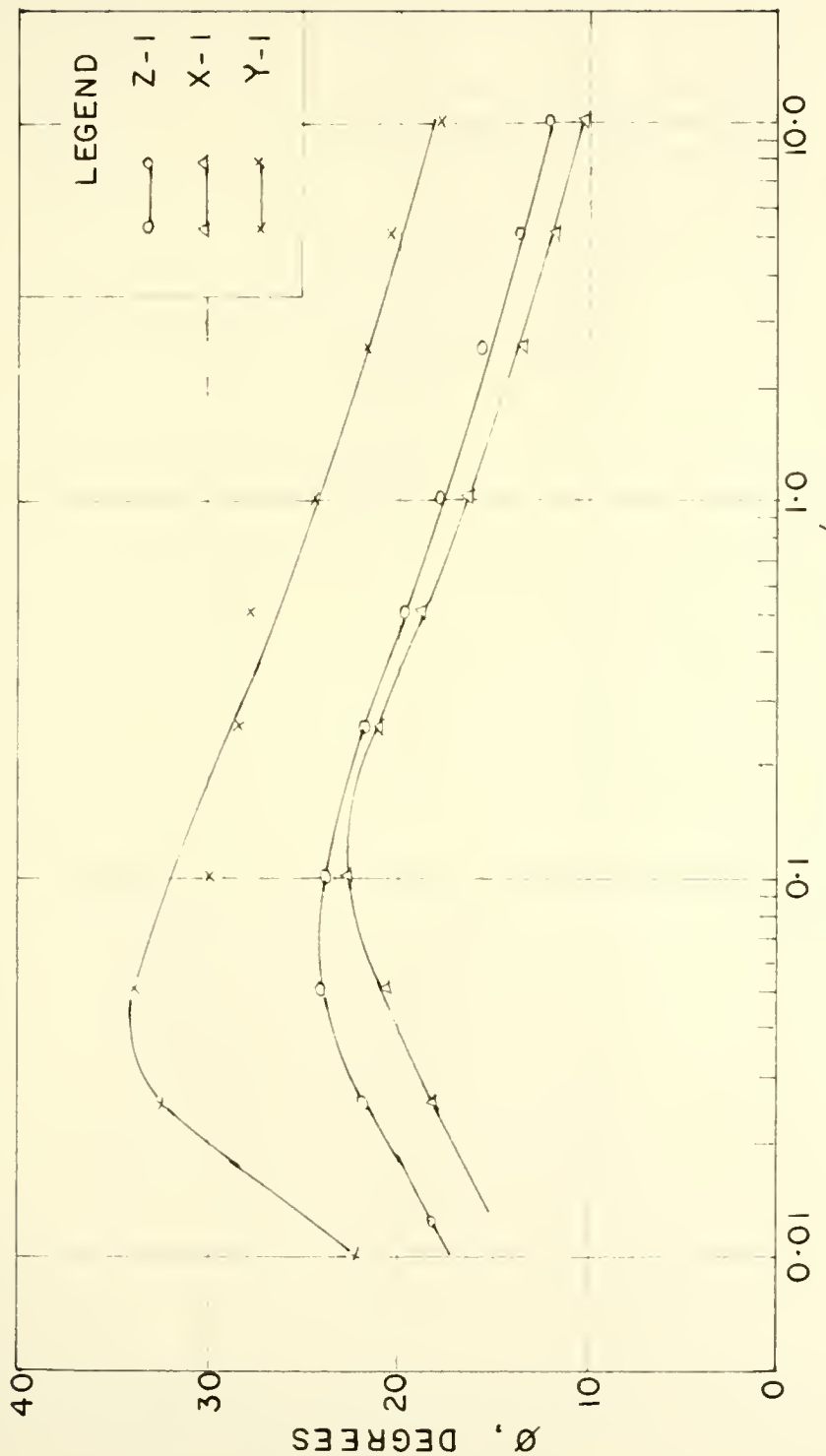

Fig. 16. Phase angle versus frequency for Mix-1 at 80°F

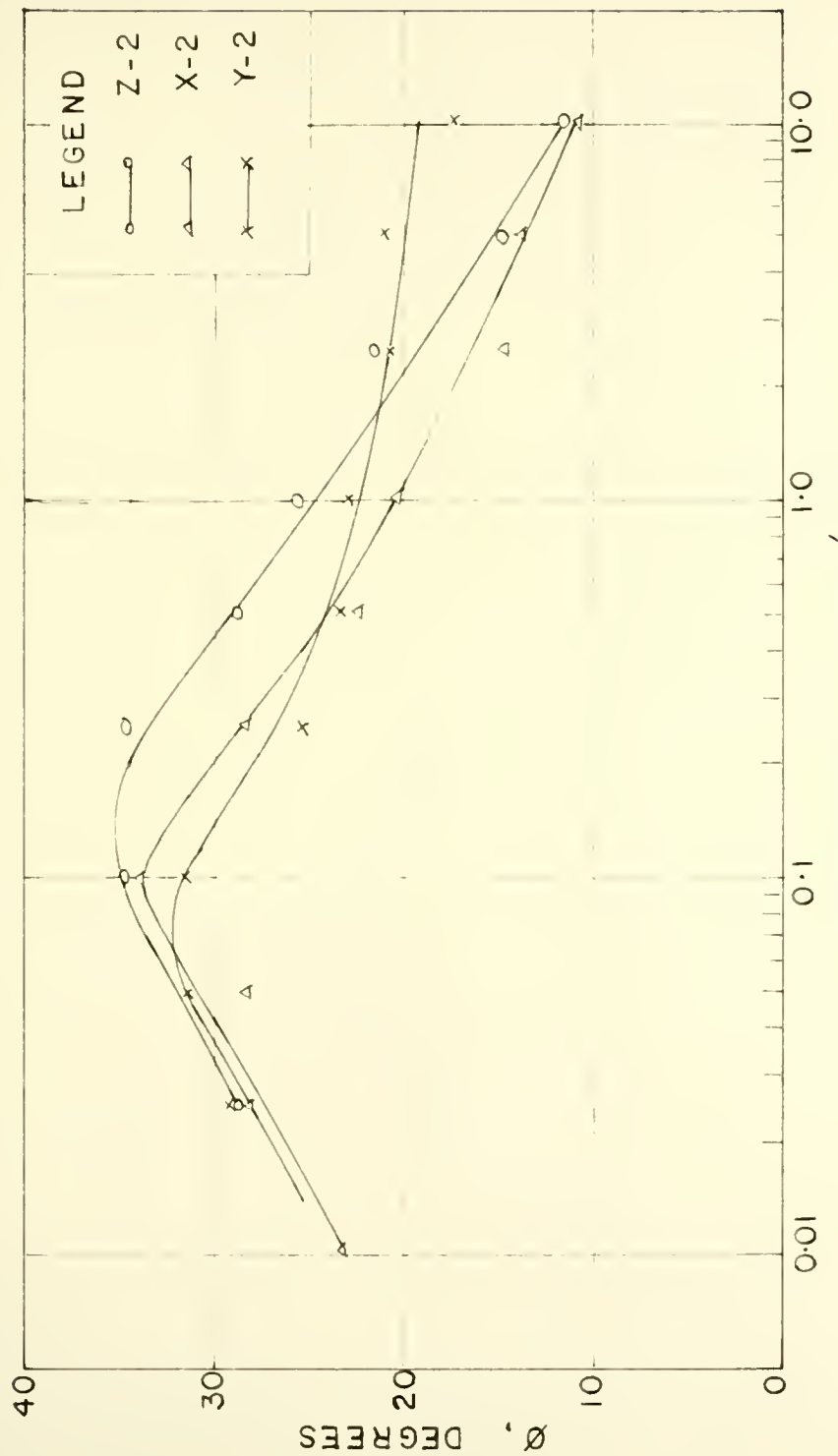

Fig. 17. Phase angle versus frequency for Mix-2 at 80°F

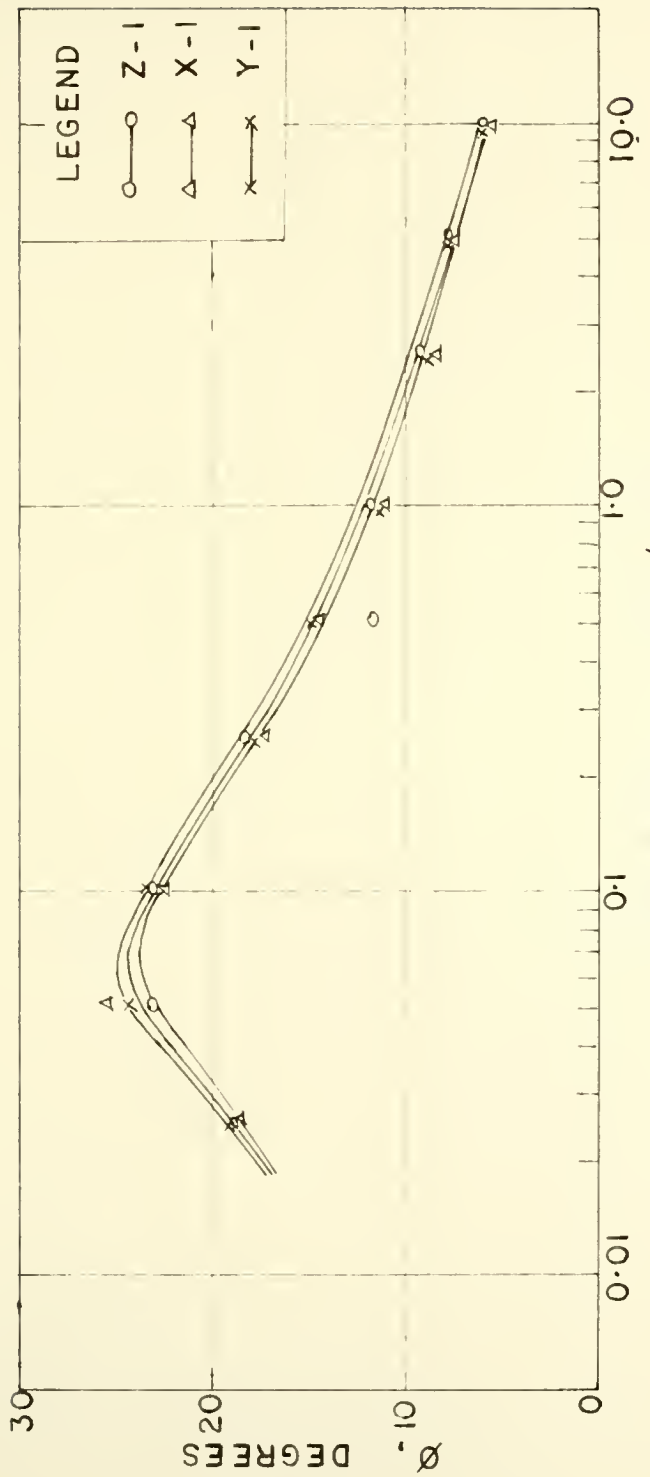

Fig. 18. Phase angle versus frequency for Mix-1 at 90°F

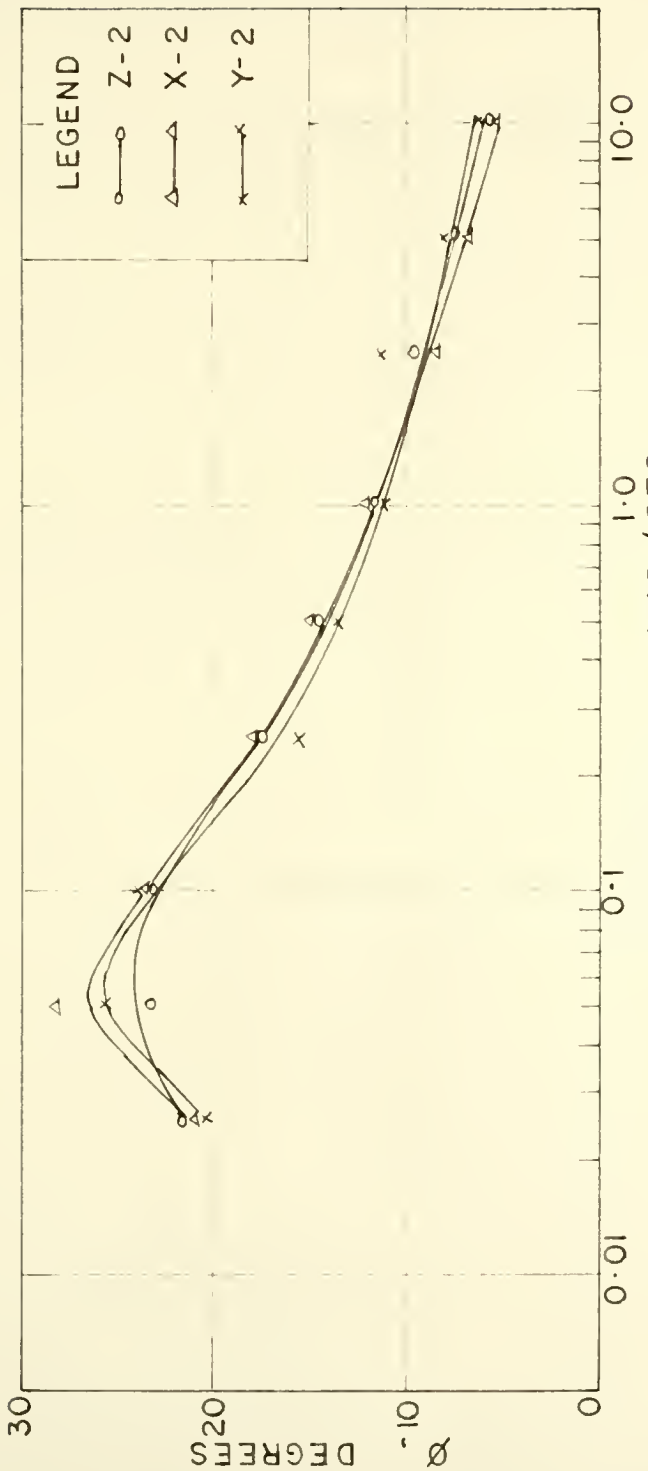

Fig. 19. Phase angle versus frequency for Mix-2 at 90°F

DISCUSSION OF RESULTS

The concept of transfer function for a given system and the methods of predicting the displacements of the system for a sinusoidal and step function input, respectively, discussed in the previous sections were applied to the analysis of the test data obtained for the two bituminous concrete mixtures. The discussion of the results are presented in this section.

Frequency Response of Asphaltic Concrete

In most of the dynamic tests a magnitude of 10 lbs. was employed for the sinusoidal load input for frequencies covering three decades, varying from 0.01 radians per second to 10.0 radians per second. These were observed to be, respectively, the slowest and the fastest frequencies to which the test specimens were responsive. The input magnitude and the output displacement were recorded in pounds and inches, respectively. Also, both of them were recorded in millivolts.

The ratio of the output to the input expressed in decibels (also referred to as amplification or gain) plotted against log frequency gives the desired frequency spectrum. The phase lag or simply the phase angle for each frequency was also computed from

$$\phi = \omega t \qquad (30)$$

where ϕ = the phase angle in radians

ω = the test frequency in rad/sec., and

t = time lag between input and output in seconds.

The phase angle is also plotted against log frequency. The two plots together represent the frequency response of the test specimen completely.

Table 10 shows typical test results for a dynamic test and Fig. 20 gives the frequency response for the same test. It is seen that the displacement of the specimen is largest at the slowest frequency and is least at the fastest frequency. Thus the gain continuously falls with increase in frequency. It was discussed before with reference to damped systems that such a curve indicates the overdamped nature of the test specimen.

The phase angle increases with increase in frequency in the first decade of test and then decreases so that a bell-shaped curve results when phase angle is plotted against frequency. The peak has, in general, been observed to occur in the region of 0.05 to 0.1 rad/sec. See Figs. 14 through 19. These results substantiate the observations of Pagen (45) and others who have studied the dynamic response of bituminous concrete. However, these investigators (43, 45, 46) have attempted to characterize the viscoelastic response of bituminous mixtures by using the phase angle and the complex elastic modulus, E^*, as obtained from the input-output traces of dynamic tests employing sinusoidal loading. This investigation is distinguished by the fact that a new approach has been taken to deal with the sinusoidal test results through the use of transfer functions to characterize the dynamic response of bituminous mixtures.

Form of the Transfer Function

From Tables 3, 4 and 5 it is seen that the transfer function derived from the frequency spectrum for each individual case is of the form

$$G(s) = \frac{A(s + a_1)(s + a_2)(s + a_3)}{(s + b_1)(s + b_2)(s + b_3)(s + b_4)} \qquad (31)$$

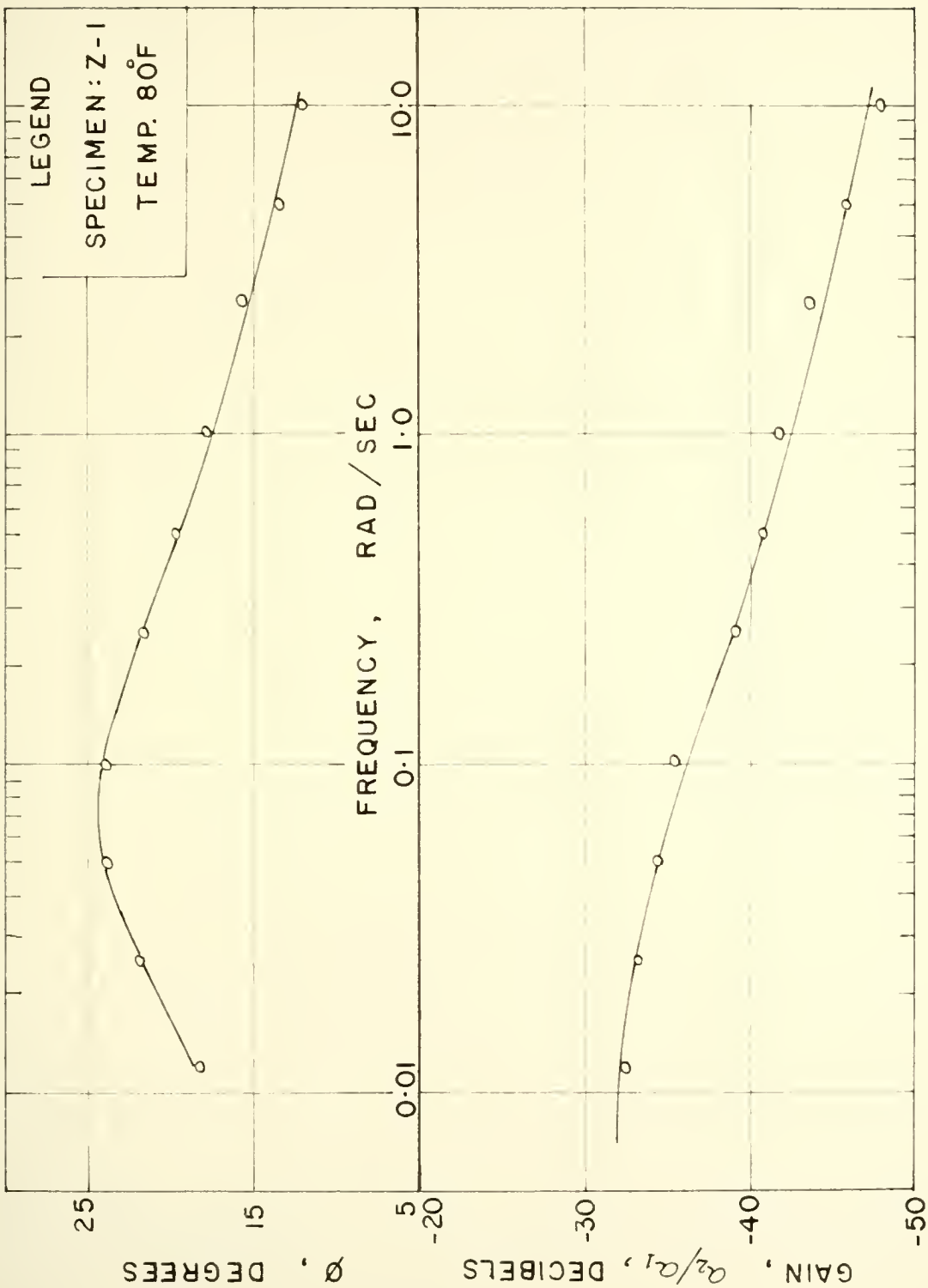

Fig. 20. Typical frequency response curve

where A is a constant and a_i 's and b_i 's are the corner frequencies as previously defined and which are obtained in the process of approximating the frequency spectrum with asymptotes. The significant feature of this form of the transfer function is that all the factors in both the numerator and denominator are to first power. It may be recalled that this is due to the geometric procedure followed in approximating the frequency spectrum with asymptotes of slopes of six decibels per octave. It was also mentioned that any slope can be used, in which case it is obvious from Eq. 29 that the transfer function may contain fraction powered or higher powered terms in either the numerator or the denominator or both. This form is not desirable since the resulting transfer function will be too difficult or even impossible to handle through Laplace transforms.

From the procedure followed in approximating the frequency spectrum with asymptotes it is obvious that the number of factors in the numerator and denominator of the transfer function in Eq. 31 depends on the number of asymptotes used to approximate the frequency spectrum. It was found from the analysis of the experimental results that the transfer function obtained using eight asymptotes was accurate enough for practical purposes, which is given in Eq. 31.

Check for the Transfer Function

From the method of obtaining the transfer function discussed under "Determination of the Transfer Function", it is obvious that the derived transfer function is simply an analytical expression for the frequency spectrum, since the asymptotic approximation is a form of curve fitting. Hence, the absolute value of the derived transfer function calculated at any frequency within the spectrum should match the corresponding value

of the gain or the ratio of the magnitude of the output a_2 to that of the input a_1, read from the curve at that frequency, that is,

$$|G(s)| = |G(j\omega)| = \frac{a_2}{a_1} \tag{32}$$

This has been checked for all the derived transfer functions and the agreement was observed to be excellent for the entire range of frequencies tested. A typical case is illustrated for specimen z-1, tested at 80°F. Table 11 gives the calculated and observed values which are plotted in Fig. 21 as a function of the frequency. Hence, it is of interest to note that the absolute value of the transfer function at a given frequency is nothing but the dimensionless output-input ratio of the system at that frequency.

It was observed from the experiments that at frequencies higher than 10 rad/sec. the output magnitude became too small to measure (the higher the frequency the smaller the output magnitude). That is, as the input frequency ω approached infinity the output magnitude a_2 approached zero, from which it follows

$$\left.\frac{a_2}{a_1}\right|_{\omega \to \infty} \approx 0 \tag{33}$$

where a_1 is the input magnitude. Hence, from Eqs. 32 and 33 it is at once seen that

$$\left.\frac{a_2}{a_1}\right|_{\omega \to \infty} = \left.|G(j\omega)|\right|_{j\omega \to \infty} = \left.|G(s)|\right|_{s \to \infty} = 0 \tag{34}$$

TABLE 11

|G(s)| and Output-Input Ratios

Specimen: z-1

Test Temperature: 80°F

$$G(s) = \frac{(0.05)(s + 0.025)(s + 0.2)(s + 2)}{(s + 0.02)(s + 0.1)(s + 1)(s + 10)}$$

ω rad/sec	$\lvert G(s) \rvert$	$R = a_2/a_1$
0.025	0.0218	0.0220
0.050	0.0192	0.0195
0.100	0.0158	0.0170
0.250	0.0120	0.0110
0.500	0.0097	0.0090
1.000	0.0077	0.0080
2.500	0.0060	0.0065
5.000	0.0046	0.0050
10.000	0.0035	0.0040

where

a_1 = input magnitude

a_2 = output magnitude

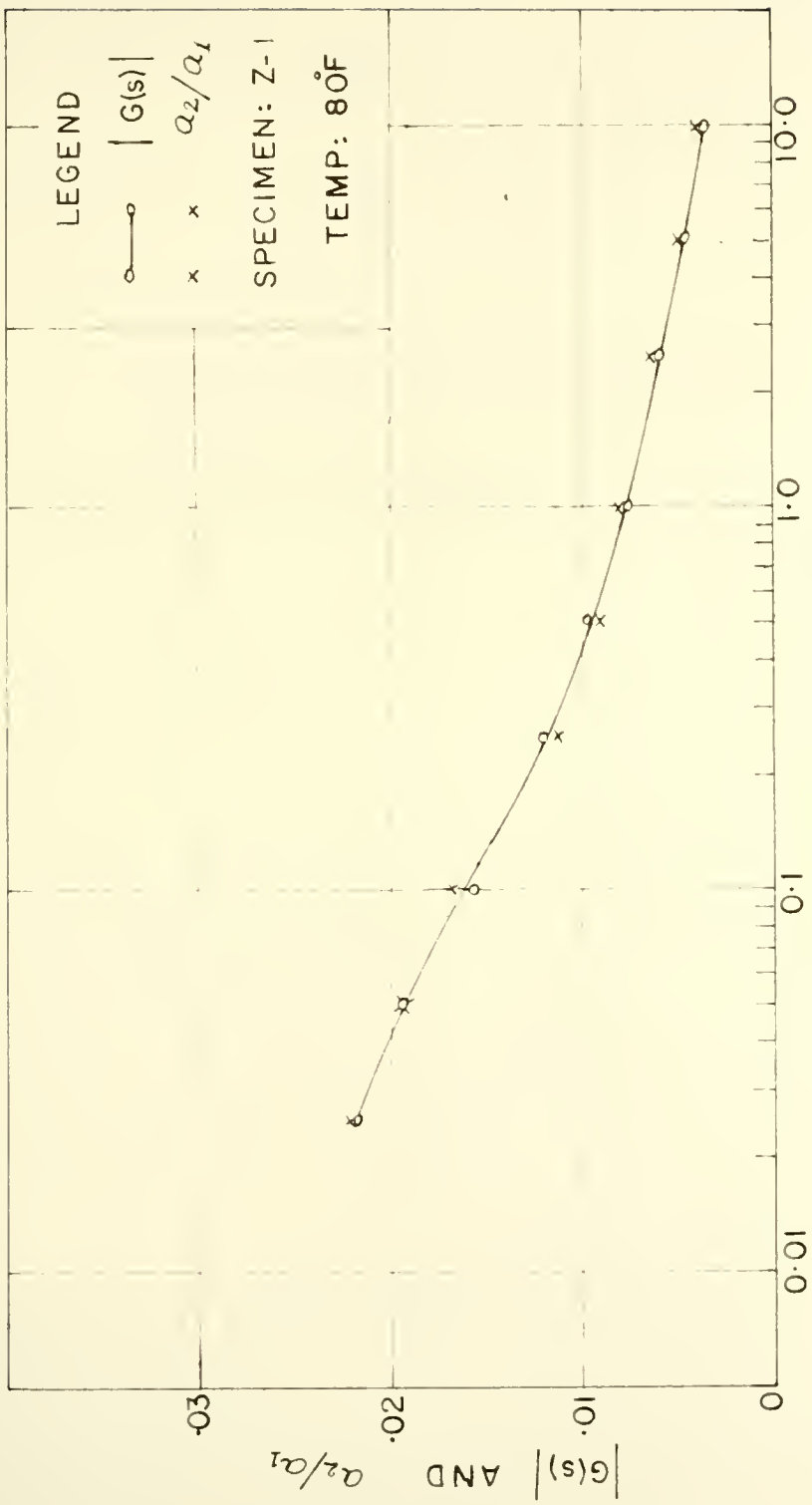

Fig. 21. Comparison of |G(s)| and Output-Input ratio

Eq. 34 offers a means of checking the validity of the experimentally derived transfer function, given by Eq. 31

$$G(s) = \frac{A(s + a_1)(s + a_2)(s + a_3)}{(s + b_1)(s + b_2)(s + b_3)(s + b_4)} \qquad (31)$$

It is easily proved that the limiting value of G(s) as $s \to \infty$ in Eq. 31 is zero.

Effect of Mix Type on Transfer Function

The two different bituminous mixes studied in this investigation were quite dissimilar in their aggregate gradings (Fig. 10) and in their binder contents, namely, 5.0% and 3.5% by weight of aggregate for Mix-1 and Mix-2, respectively. However, it is apparent from Fig. 22 that there was no appreciable difference in the transfer functions of the specimens, irrespective of their composition or orientation when tested at any one temperature. Even though the grading and asphalt content were different for the two mixes, their density-void ratio characteristics were similar, namely, 142.6 pcf and 6.5% for Mix-1 and 142.0 pcf and 8.5% for Mix-2.

It can be anticipated that density will have a marked influence on the response to loading of a given mix and hence on its transfer function. However, more work is necessary to study the effect of this and other mix variables.

Effect of Specimen Orientation

It was pointed out under "Experimental Investigation", that for each mix three specimens were cut along three mutual perpendicular directions, designated x, y and z. It is seen from Fig. 22 that there is not much

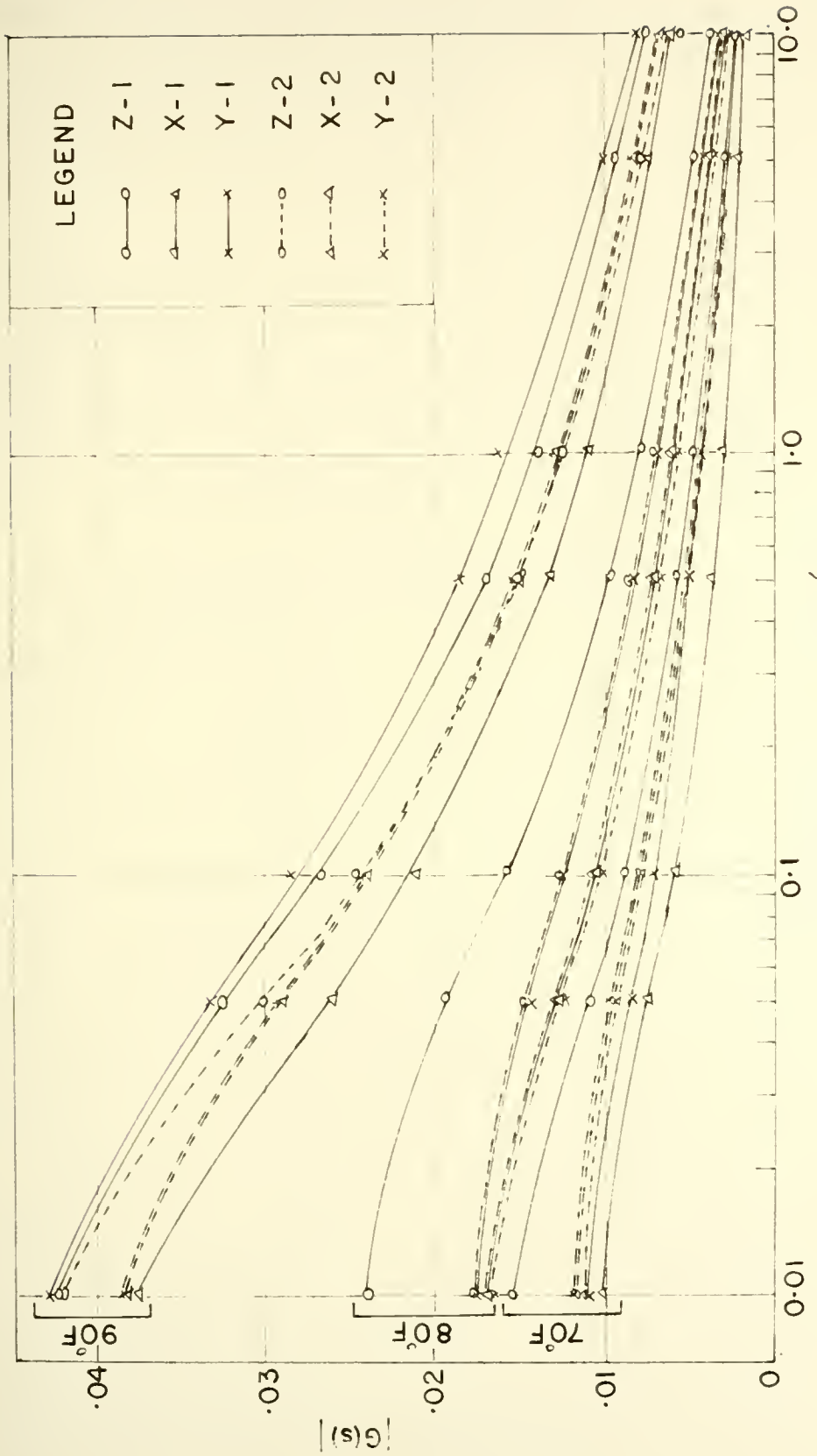

Fig. 22. Curves of $|G(s)|$ versus frequency

difference in the transfer functions of the differently oriented specimens of either mix at any one temperature. This suggests that effect of anisotropy, if any, is not reflected in the transfer function.

This is contrary to the observations of Busching (35) who noted differences in response of differently oriented specimens prepared in the same manner as in the present investigation, though for static loads. One possible explanation is that the stress levels he applied to the specimens, namely, 23.1, 40.8 and 58.3 psi were much higher than the stress level of 10.0 psi used in the present study.

Effect of Temperature

The experiments in the present investigation were conducted at 70°, 80°, and 90°F. By examining the absolute value curves in Fig. 22, it is readily seen that temperature plays an important role in the transfer function of any given specimen. Asphalt cement being thermoplastic, the asphaltic concrete specimen will yield increased displacements for increases in temperature at a given stress level. This results in a decrease in viscosity of the binder in the asphaltic concrete as temperature increases. Thus the output-input ratio for a constant input at any frequency will increase with decrease in viscosity, or increase in temperature. This is precisely what is shown by the curves.

Examination of the transfer functions in Tables 3, 4, and 5 reveals that, for a given specimen, the various factors in the numerator and denominator do not seem to vary much with change in temperature, but that the coefficient A varies appreciably. It would be of interest to study this change in A with reference to the viscosity of asphalt cement or the asphalt cement-filler matrix. This is suggested for further study.

Effect of Specimen Size on Transfer Function

Frequency-response tests were conducted on three different-sized specimens with constant height-width ratio using Mix-1 at 90°F. They were all cut along the same direction in the compacted beam. The large, medium and small sizes were 1 1/4" x 1 1/4" x 2 1/2", 1" x 1" x 2" and 3/4" x 3/4" x 1 1/2", respectively. Their frequency spectrums are shown in Fig. 23, and the transfer function is given in Table 12. The absolute value curve for the derived transfer function and the output-input ratio curves for the three specimens are shown in Fig. 24.

From Fig. 23 it is seen that the frequency spectrums for the three specimens are nearly the same and that they can be approximated by one single transfer function. The absolute value curve for this transfer function and the output-input ratio curves for the three specimens plotted in Fig. 24 confirm that the transfer function is independent of the specimen size, since all of them fall on the same curve.

In the light of this observation, it appears that the transfer function can be used to represent the dynamic characteristics of a viscoelastic material in much the same way as the elastic modulus represents the stress-strain characteristics of an elastic material. In other words, for a given viscoelastic material such as a bituminous concrete there will be only one transfer function for a given temperature.

Prediction of Displacements for Sinusoidal Loads

The discussions so far have indicated the general validity of the transfer function for bituminous concrete as derived from dynamic tests. It was seen under "Related Theory" that once the transfer function of a system is known, it can be used to predict the output of the system for

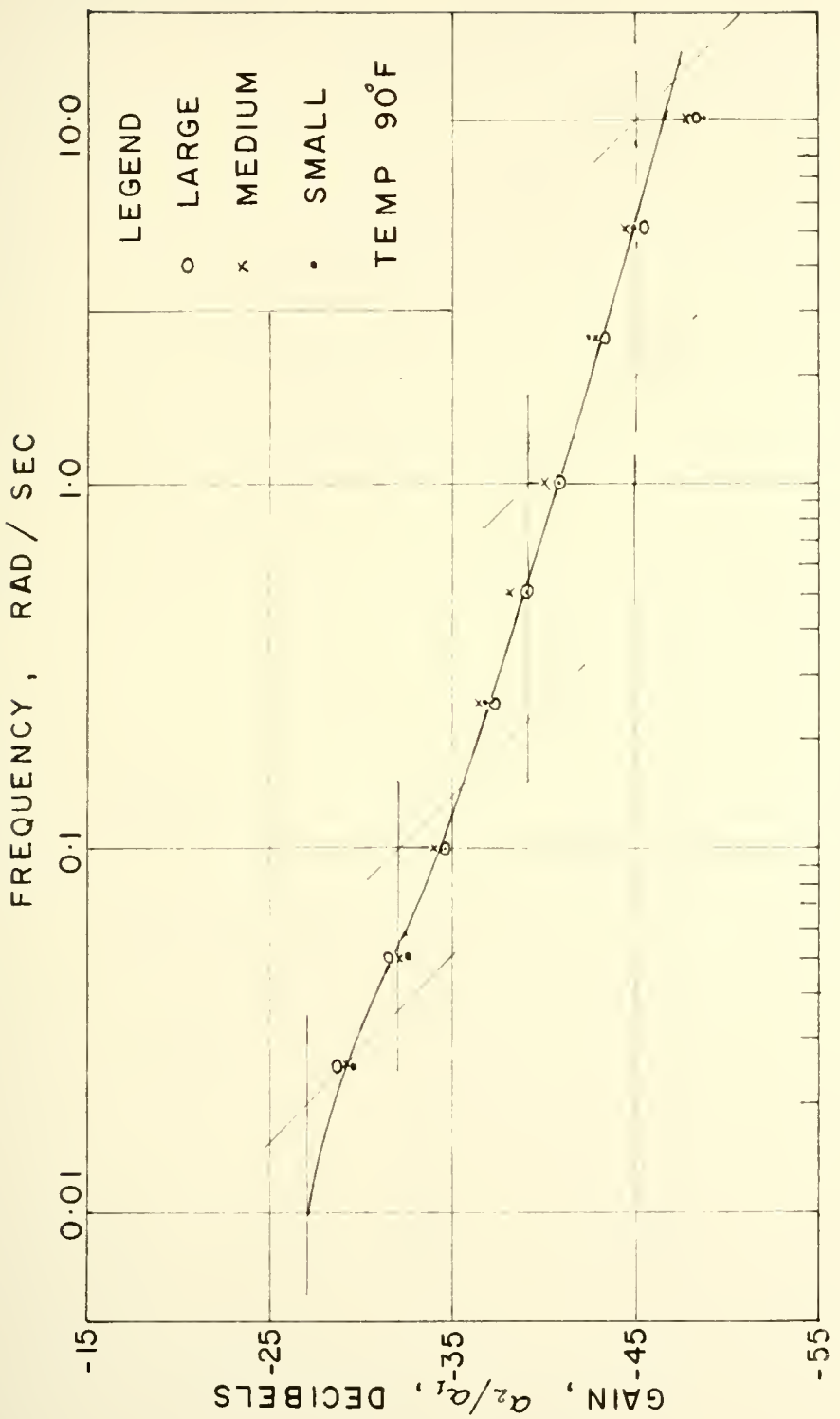

Fig. 23. Specimen size and the frequency spectrum

TABLE 12

Effect of Specimen Size

LEGEND

Large: 1 1/4" x 1 1/4" x 2 1/2"

Medium: 1" x 1" x 2"

Small: 3/4" x 3/4" x 1 1/2"

Mixture: Mix-1

Test Temperature: 90°F

$$G(s) = \frac{(0.055)(s + 0.035)(s + 0.23)(s + 2)}{(s + 0.02)(s + 0.1)(s + 1)(s + 10)}$$

Calculated and Measured Displacements
for Constant Loads

Specimen	f_o	p	x(t)	
			Calculated	Measured
	lbs	psi	inch($\times 10^{-4}$)	inch($\times 10^{-4}$)
Large	3.9	2.5	4.32	4.00
	7.8	5.0	8.64	7.50
	15.6	10.0	17.28	16.25
Medium	2.5	2.5	2.76	2.25
	5.0	5.0	5.52	3.75
	10.0	10.0	11.04	10.00
Small	2.8	5.0	3.10	2.00
	5.6	10.0	6.20	3.75
	11.2	20.0	12.40	10.00

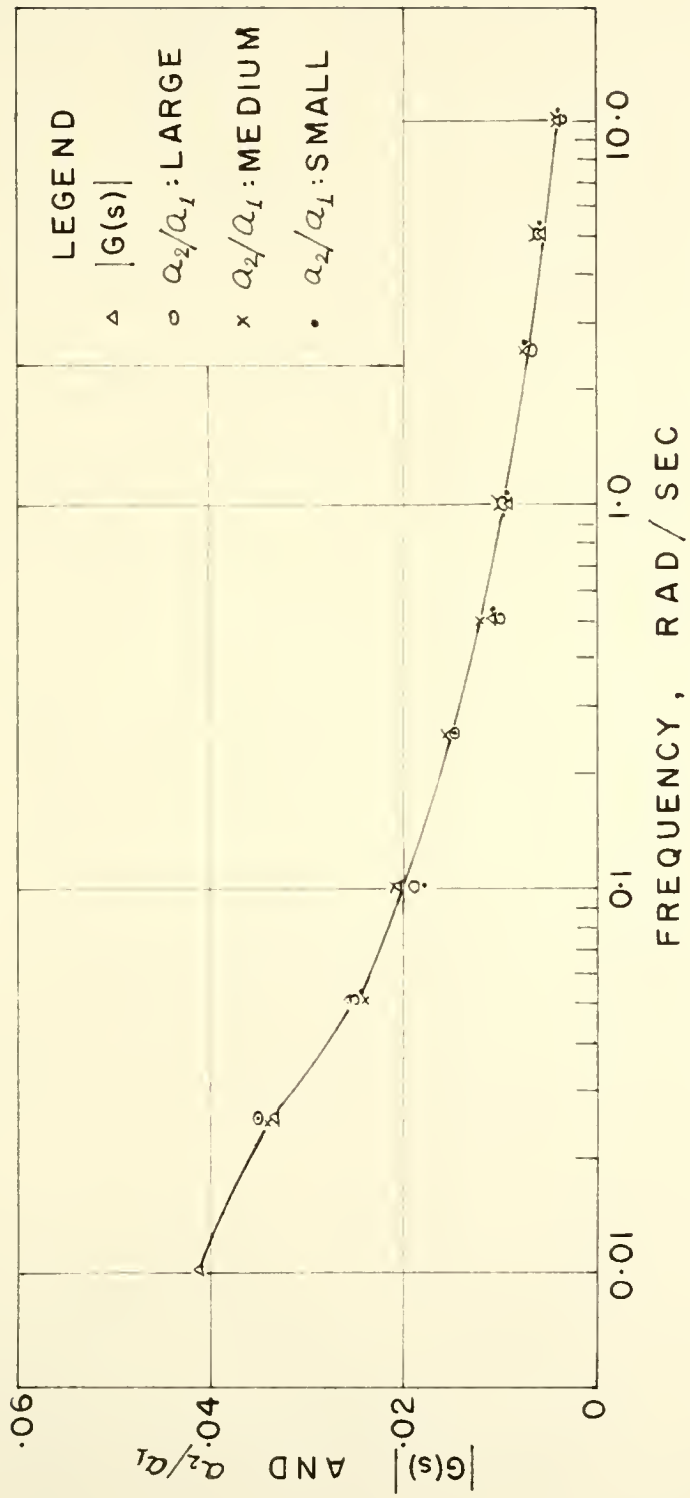

Fig. 24. Specimen size and |G(s)|

any given input which is a function of time. After the transfer functions for the asphaltic concrete test specimens under investigation were determined, attempts were made to predict the output displacement of the specimens when subjected to a sinusoidal load input of known magnitude and frequency. Each specimen was tested under three sinusoidal inputs at each of the three temperatures used previously.

As previously indicated, the solution for the output displacement of a dynamic system with a transfer function G(s) for a sinusoidal load input is given by

$$x(t) = f_o|G(s)| \sin(\omega t + \phi) \qquad (20)$$

where f_o = magnitude of the input

ω = frequency of the input

ϕ = phase angle between output and input.

In Eq. 20, $x(t)$ is a maximum when $\sin(\omega t + \phi) = 1$, so that

$$x(t)_{max} = f_o|G(s)| \qquad (35)$$

Experimentally, it is convenient to measure $x(t)_{max}$ at the peak of the sinusoidal displacement output. Thus, the calculated displacement from Eq. 35 can be compared with the measured displacement for a given magnitude and frequency.

It was mentioned elsewhere that in the experimental set-up of this investigation, the input was recorded in pounds and millivolts and the output was recorded in inches and millivolts. Thus the output-input ratio can be either dimensionless or in units of inch per pound. The frequency spectrum and the transfer function analyses were obtained as dimensionless

quantities. In applying units to Eq. 35, an experimental constant K needs to be introduced and it becomes

$$x(t)_{max} = K f_o |G(s)| \qquad (36)$$

From the sensitivity control values of the recorder, K was calculated and found to be

$$K = 25 \times 10^{-4} \text{ inch/pound.} \qquad (37)$$

The calculated and measured values for the maximum displacement for all the specimens are shown in Tables 6, 7 and 8. In all cases the magnitude of the sinusoidal input was kept the same and only the frequency was varied. Comparison of the calculated and the measured displacement values clearly indicates the close agreement between these values in all cases. Besides proving the efficacy of the transfer function as a displacement predicting tool for viscoelastic materials, this also shows that the bituminous concrete behaves as a linear system at the levels of stress considered in the tests.

Prediction of Displacements for Static Loads

As was discussed under "Related Theory", the transfer function can be used to predict the time-dependent displacements of a system subjected to a step function input and a static load can be treated as a step function. The solution for the displacement was shown to be

$$x(t) = C_1 e^{b_1 t} + C_2 e^{b_2 t} + C_3 e^{b_3 t} + C_4 e^{b_4 t} + C_5 \qquad (27)$$

where C_i 's are constants for the system as defined earlier and b_i 's are

the roots of the denominator of the transfer function which are observed to be negative in the case of the experimentally derived transfer functions.

Two boundary conditions are applicable to Eq. 27: 1) when $t = 0$, 2) when $t = \infty$.

When $t = 0$,

$$x(t) = 0 \tag{38}$$

that is

$$C_5 = C_1 + C_2 + C_3 + C_4. \tag{39}$$

When $t = \infty$,

$$x(t) = C_5 \tag{40}$$

When a constant load is applied to a viscoelastic material, the displacement approaches a constant value after a certain time depending upon the nature of the material. In the laboratory, for the bituminous concrete specimens tested, this time was observed to be in the order of a few minutes. Hence, the second boundary condition discussed above can be applied to this steady displacement value in the test, that is, Eq. 40 can be used to calculate the displacement. The limitations of using Eq. 40 are recognized in that in a test t does not reach ∞ and hence the measured value will be slightly lower than the calculated value.

In order to get the calculated displacement in proper units, Eq. 40 should be multiplied by the experimental constant, described in the previous section so that

$$x(t) = K\, C_5 \tag{41}$$

where $K = 25 \times 10^{-4}$ inch/pound. C_5 has the units of pound.

The calculated and measured values of the displacement at three temperatures for all the specimens, each under three different constant loads, are shown in Tables 6, 7 and 8. Comparison of the calculated and the measured displacement values clearly indicates the close agreement between the two in almost all cases. This observation is very significant and it brings to focus the following points:

1. The mathematical theory of transfer functions is applicable to viscoelastic materials in general, and to bituminous concrete in particular.

2. The techniques developed to derive the transfer function in this investigation are sound.

3. The transfer function serves as a connecting link between the responses of the material tested under dynamic and static loads.

Differential Equation from Transfer Function

Once the transfer function is known for a given system, the differential equation for the system behavior can be written using the Laplace inverse transform. For bituminous concrete, the transfer function is of the form

$$G(s) = \frac{A(s + a_1)(s + a_2)(s + a_3)}{(s + b_1)(s + b_2)(s + b_3)(s + b_4)} \qquad (31)$$

From definition

$$G(s) = \frac{\bar{x}(s)}{\bar{f}(s)} \qquad (10)$$

where $\bar{x}(s)$ = operational output = $\mathcal{L}\{x(t)\}$

$\bar{f}(s)$ = operational input = $\mathcal{L}\{f(t)\}$

From Eqs. 10 and 31,

$$\frac{\bar{x}(s)}{\bar{f}(s)} = \frac{A(s + a_1)(s + a_2)(s + a_3)}{(s + b_1)(s + b_2)(s + b_3)(s + b_4)} \qquad (42)$$

Rewriting,

$$\bar{x}(s)(s + b_1)(s + b_2)(s + b_3)(s + b_4) = A\,\bar{f}(s)(s + a_1)(s + a_2)(s + a_3) \qquad (42.1)$$

Multiplying and rearranging the terms,

$$\bar{x}(s)[s^4 + B_1s^3 + B_2s^2 + B_3s + B_4] = A\,\bar{f}(s)[s^3 + B_5s^2 + B_6s + B_7] \qquad (43)$$

where $B_1 = b_1 + b_2 + b_3 + b_4$ (44)

$B_2 = b_1b_2 + b_2b_3 + b_3b_4 + b_4b_1 + b_4b_2 + b_3b_1$ (45)

$B_3 = b_1b_2b_3 + b_2b_3b_4 + b_3b_4b_1 + b_4b_1b_2$ (46)

$B_4 = b_1b_2b_3b_4$ (47)

$B_5 = a_1 + a_2 + a_3$ (48)

$B_6 = a_1a_2 + a_2a_3 + a_3a_1$ (49)

$B_7 = a_1a_2a_3$ (50)

Rewriting Eq. 43,

$$s^4\bar{x}(s) + B_1s^3\bar{x}(s) + B_2s^2\bar{x}(s) + B_3s\bar{x}(s) + B_4\bar{x}(s)$$

$$= A[s^3\bar{f}(s) + B_5s^2\bar{f}(s) + B_6s\bar{f}(s) + B_7\bar{f}(s)] \qquad (43.1)$$

Applying the Laplace inverse transform,

$$\frac{d^4x(t)}{dt^4} + B_1\frac{d^3x(t)}{dt^3} + B_2\frac{d^2x(t)}{dt^2} + B_3\frac{dx(t)}{dt} + B_4x(t)$$

$$= A\left[\frac{d^3f(t)}{dt^3} + B_5\frac{d^2f(t)}{dt^2} + B_6\frac{df(t)}{dt} + B_7f(t)\right] \qquad (51)$$

Eq. 51 is a fourth order linear differential equation with constant coefficients which describes the dynamics of the bituminous concrete. The input (force) and the output (displacement) are the two variables in the equation which are functions of time. The constants B_i 's are easily determined from the roots of the denominator and the numerator of the transfer function.

In dynamical systems, if the roots of the denominator of the transfer function are real and distinct, then the system is overdamped (41). For the bituminous concrete under investigation the four roots, $-b_1$, $-b_2$, $-b_3$ and $-b_4$, are real and distinct, which indicates that the bituminous concrete is an overdamped system.

The constants, B_1 through B_7, were calculated for each specimen tested at each temperature. They are shown in Table 13. It is of significance to note here that the roots of the differential equation are obtained as the corner frequencies directly from the frequency spectrum for the material under test, and no assumption whatsoever has been made in deriving the equation.

TABLE 13

Constants of the Differential Equation

Temp °F	Specimen	A	B_1	B_2	B_3	B_4	B_5	B_6	B_7
70	z-1	0.035	11.120	11.322	1.222	0.020	1.911	0.364	0.009
	x-1	0.024	11.114	11.266	1.166	0.015	1.800	0.323	0.006
	y-1	0.035	12.270	23.245	5.460	0.100	3.130	1.173	0.032
	z-2	0.032	11.120	11.322	1.222	0.020	1.985	0.337	0.007
	x-2	0.035	11.120	11.322	1.222	0.020	1.785	0.300	0.006
	y-2	0.035	11.120	11.322	1.222	0.020	1.785	0.300	0.006
80	z-1	0.050	11.120	11.322	1.222	0.020	2.225	0.455	0.010
	x-1	0.041	11.120	11.322	1.222	0.020	1.998	0.361	0.008
	y-1	0.040	11.120	11.322	1.222	0.020	2.485	0.489	0.009
	z-2	0.040	11.120	11.322	1.222	0.020	2.485	0.489	0.009
	x-2	0.041	11.120	11.322	1.222	0.020	1.998	0.361	0.008
	y-2	0.041	11.120	11.322	1.222	0.020	1.998	0.361	0.008
90	z-1	0.100	11.115	11.266	1.166	0.015	1.920	0.378	0.006
	x-1	0.082	11.120	11.322	1.222	0.020	1.830	0.374	0.009
	y-1	0.100	11.115	11.266	1.666	0.015	2.190	0.383	0.007
	z-2	0.070	11.120	11.322	1.222	0.020	2.700	0.505	0.012
	x-2	0.085	11.115	11.266	1.166	0.015	2.020	0.400	0.007
	y-2	0.085	11.115	11.266	1.166	0.015	2.020	0.400	0.007

Elastic Modulus from Transfer Function

The differential equation that was obtained for the bituminous concrete using the transfer function relates the two time-dependent variables, force and displacement. If the relationship is assumed to be time independent, as in an elastic analysis, then the time derivatives of x and f drop off in Eq. 51, and

$$B_4 x = AB_7 f \tag{52}$$

where x = displacement,

f = applied force,

A, B_4, and B_7 are constants as determined before.

Eq. 52 gives the force-displacement ratio as

$$\frac{f}{x} = \frac{B_4}{AB_7} \tag{53}$$

From Eq. 53, the stress-strain ratio can be computed for the material to give the elastic modulus.

In this investigation, the gage length of the specimen was two inches and the area of the specimen on which force was applied was one square inch. Hence, the elastic modulus E is obtained from

$$E = \frac{\text{stress}}{\text{strain}} = \frac{f}{x/2} \text{ psi.} \tag{54}$$

Substituting Eq. 54 into Eq. 53, and using the experimental constant to get the proper units,

$$E = \frac{2B_4}{KAB_7} \text{ psi} \tag{55}$$

where $K = 25 \times 10^{-4}$ inch/psi. It may be noted that K is in units of inch/psi in this case because of the area of the test specimen being one square inch where the applied load in pounds was considered as the applied stress in psi.

It is of interest to note that Eq. 55 involves only the use of constants determined in the transfer function analysis for the material under test. Hence, if the differential equation derived from the transfer function analysis is considered as the viscoelastic representation of the material, then it automatically includes the elastic case which is only a special case of the problem.

Using Eq. 55 the elastic modulus was calculated for each specimen at each temperature. The results are summarized in Table 14. The values are comparable to those found in the literature for bituminous concrete (35, 42). With respect to the temperature of test, the elastic modulus decreases with increase of temperature which should be the case because of the decrease of the viscosity of the binder with increase in temperature. At any given temperature, the orientation of the specimen does not seem to affect the elastic modulus.

It was observed previously that the mix type did not seem to have appreciable influence on the transfer function, due possibly to similarity in density-void ratio. The results of Table 14 clearly show that this holds for the elastic modulus also.

TABLE 14

Values of Elastic Modulus

Specimen	E in psi @ 70°F	@ 80°F	@ 90°F
z-1	5.05×10^4	3.20×10^4	2.00×10^4
x-1	6.68 "	4.82 "	2.18 "
y-1	7.13 "	4.45 "	1.72 "
z-2	7.15 "	4.45 "	1.82 "
x-2	7.50 "	4.82 "	2.02 "
y-2	7.50 "	4.81 "	2.02 "

CONCLUSIONS

In this study specimens of asphaltic concrete cut from laboratory-compacted beams of two different compositions were tested both statically and dynamically at three test temperatures. Based on the results and within the limitations of this investigation, the following conclusions are enumerated:

1. The viscoelastic or time-dependent characteristics of an asphaltic concrete can be represented by a transfer function G(s) which is a function of the complex variable s. The transfer function is unique for the material at a given temperature. It is possible to obtain this function experimentally from a series of sinusoidal load tests on the material.

2. The transfer function for an asphaltic concrete is of the form

$$G(s) = \frac{A(s + a_1)(s + a_2)(s + a_3)}{(s + b_1)(s + b_2)(s + b_3)(s + b_4)} \qquad (31)$$

where A is a constant, and a_i 's and b_i 's are roots of the numerator and denominator, respectively.

3. The roots of the denominator of G(s), namely b_1, b_2, b_3 and b_4, are real and distinct, thus indicating that bituminous concrete behaves as an overdamped system.

4. Parameters obtained in the transfer function for bituminous concrete are believed to be better indicators of material performance than those commonly used, such as, Young's modulus, Poisson's ratio, etc.

which change with rate and time of loading.

5. Temperature is the one single factor which has the greatest effect on the transfer function of asphaltic concrete. Increase in temperature increases the value of the constant A in the transfer function equation.

6. The transfer function is a powerful tool useful in predicting the displacement of asphaltic concrete under an applied load, dynamic or static. By treating the static load as a step function of time, the resulting displacement can be calculated by means of the transfer function derived experimentally from the dynamic test. The excellent agreement between the calculated and measured values of the displacement in this investigation validates the concept that the transfer function represents a material property which is independent of the type of load input.

7. Through the use of the transfer function and without assuming any spring-dashpot model, it is possible to represent the time-dependent behavior of asphaltic concrete by a fourth order linear differential equation with constant coefficients. The coefficients can be computed from the roots of the denominator and numerator of the transfer function.

8. It is possible to determine the elastic modulus of asphaltic concrete, assuming it as an elastic system, through the differential equation discussed above by setting all the time derivatives to zero. The range of values thus calculated for all the specimens in this investigation appears reasonable in the light of values obtained by other investigators.

SUGGESTIONS FOR FURTHER RESEARCH

In attempting to apply the concept of transfer functions to practical problems, the limitations of this investigation should be borne in mind. The present investigation is a first step in formulating and testing the concept under controlled laboratory conditions, assuming that the bituminous concrete behaves as a linear system. The levels of applied stress and the resulting small displacements were limiting factors in the laboratory investigation. The conditions in full-scale field problems are considerably different from those in the laboratory and it can not be assumed that the transfer function value determined from limited laboratory testing will be specifically applicable to all field conditions. Pilot investigations under full-scale field conditions are, therefore, necessary to establish the validity of the transfer function concept for analysis of problems of practical interest.

As a further application of the transfer function in the laboratory investigation attempts were made to predict the displacement of the asphaltic concrete test specimens subjected to shock loads. A weight of 500 grams was dropped on the specimen from a height of four inches and the displacement of the specimen during the impact was recorded by a Beckman electronic recorder using an LVDT as the sensing device. Considering the force due to the impact, f_I, as a Dirac impulse function, the displacement was calculated from Eq. 12

$$x(t) = \mathcal{L}^{-1}\{G(s)\ \bar{f}(s)\} \tag{12}$$

where G(s) is the transfer function of the bituminous concrete and $\bar{f}(s)$ is the Laplace transform of the force due to impact, which is f_I itself, that is

$$\bar{f}(s) = f_I \tag{56}$$

Using the method of partial fractions the soltuion for x(t) was obtained as

$$x(t) = C_1 e^{-b_1 t} + C_2 e^{-b_2 t} + C_3 e^{-b_3 t} + C_4 e^{-b_4 t} \tag{57}$$

where C_i 's are constants independent of t and b_i 's are the roots of the denominator of the transfer function G(s).

Though the calculated and measured values of the displacements agreed reasonably well in some cases, in general the agreement was poor. This was considered mainly due to the lack of a well-designed shock loading apparatus capable of producing reproducable loads. However, the general trend of the test results strongly indicated that with further improvement in the shock testing procedure, better agreement might be expected between the measured values and those calculated using transfer functions. This is suggested for further research.

In this investigation attempts also were made to measure the displacement of the test specimen in the x and y directions, both for the static and sinusoidal load inputs. It was observed that in a sinusoidal load test the output displacements in the lateral directions were also

BIBLIOGRAPHY

sinusoidal, but the magnitude of the output traces in these directions was too small for meaningful interpretation. However, by the use of an electronic recorder with greater amplification than the one used in this study it should be possible to get enlarged output traces. Then from the input-output data of the test specimen a transfer function could be derived for each direction, say $G(s)_x$, $G(s)_y$ and $G(s)_z$, the input being the same for all the three cases. It would be of interest to study the relationship among these three transfer functions in order to throw more light on the use of transfer functions to characterize material behavior. This, again, is suggested for further research.

In addition, the following suggestions are offered for extension of this investigation to studies which will contribute understanding for the use of transfer functions in the structural design of pavements.

1. The effects on the transfer function of viscosity of the asphalt cement and the density of a bituminous mix need to be studied in detail, since this would lead to a better understanding of the viscoelastic characteristics of the mix itself, and thus possibly to a rational mix design.

2. The concept of transfer functions can be extended to a layered system such as an asphaltic concrete beam or a slab supported on springs or on actual base course materials. The laboratory evaluation of the transfer function for such a system would pave the way for a full-scale pavement analysis in the field.

3. Soil and concrete are the other pavement materials to which the transfer function analysis can be logically extended. Since the rheological behavior of clay soils has been studied widely, it would be of interest to apply the transfer function concept to them. It is probable

that their mechanistic behavior could be better understood through the use of transfer functions.

4. The analysis in this investigation has been based on the assumption on linearity. However, pavement materials do not always conform to this assumption, and hence, it would be logical to study the nonlinear transfer functions in these cases. Such an analysis should place the structural design of pavements on a more rational basis.

BIBLIOGRAPHY

1. Highway Research Board, The AASHO Road Test, Report No. 5, Pavement Research (Special Report 61E), 1962.

2. The Asphalt Institute, Mix Design Methods for Asphalt Concrete (MS-2) 1963.

3. Westergaard, H. M., "Stresses in Concrete Pavements Computed by Theoretical Analysis," Public Roads, Vol. 7, 1926.

4. Hogg, A. H. A., "Equilibrium of a Thin Plate, Symmetrically Loaded, Resting on an Elastic Foundation of Infinite Depth," Philosophical Magazine, Vol. 25, 1928.

5. Burmister, D. M., "The Theory of Stresses and Displacements in Layered Systems and Application to Design of Airport Runways," Proceedings, Highway Research Board, Vol. 23, 1943.

6. Fox, L., "Computation of Traffic Stresses in a Simple Road Structure," Proceedings, Second International Conference on Soil Mechanics, Vol. 2, Rotterdam, 1948.

7. Acum, W. E. A., and Fox, L., "Computation of Load Stresses in a Three-Layer Elastic System," Geotechnique, Vol. II, 1951.

8. Burmister, D. M., "The General Theory of Stresses and Displacements in Layered Systems, " Journal of Applied Physics, Vol. 16, 1945.

9. Schiffman, R. L., "The Numerical Solution for Stresses and Displacements in a Three-layer Soil System," Proceedings, Fourth International Conference on Soil Mechanics and Foundations, Vol. 2, 1957.

10. Mehta, M. R., and Veletsos, A. S., "Stresses and Displacements in Layered Systems," Structural Research Series, No. 178, University of Illinois, 1959.

11. Lee, E. H., "Stress Analysis in Viscoelastic Bodies," Quarterly of Applied Mathematics, July 1955.

12. Biot, M. A., "Theory of Stress-Strain Relations in Anisotropic Viscoelasticity and Relaxation Phenomena," Journal of Applied Physics, Vol. 25, No. 11, November 1954.

13. Terzaghi, K., "The Static Rigidity of Plastic Clays," Journal of Rheology, Vol. 2, No. 3, July 1931.

14. Mack, C., "Rheology of Bituminous Mixtures Relative to the Properties of Asphalts," Proceedings, Association of Asphalt Paving Technologists, Vol. 13, 1942.

15. Biot, M. A., "Dynamics of Viscoelastic Anisotropic Media," Proceedings, Fourth Midwestern Conference on Solid Mechanics, September 1955.

16. Lee, E. H., "Viscoelastic Stress Analysis," Structural Mechanics, Proceedings, First Symposium on Naval Structural Mechanics, Pergamon Press, New York, 1960.

17. Lee, E. H., and Rogers, T. G., "Solution of Viscoelastic Analysis Problems Using Measured Creep or Relaxation Functions," Journal of Applied Mechanics, Vol. 30, No. 1, March 1963.

18. Freudenthal, A. M., and Lorsch, H. G., "The Infinite Elastic Beam on a Linear Viscoelastic Foundation," Journal of the Engineering Mechanics Division, Proceedings, A.S.C.E., Vol. 83, No. EM 1, January 1957.

19. Pister, K. S., and Monismith, C. L., "Analysis of Viscoelastic Flexible Pavements," Flexible Pavement Design Studies 1960, Highway Research Bulletin 269, 1960.

20. Pister, K. S., and Westmann, R. A., "Analysis of Viscoelastic Pavements Subjected to Moving Loads," Proceedings, International Conference of the Structural Design of Asphalt Pavements, University of Michigan, 1963.

21. Hoskin, B. C. and Lee, E. H., "Flexible Surfaces on Viscoelastic Subgrades," Journal of the Engineering Mechanics Division, Proceedings, A.S.C.E., Vol. 85, No. EM 4, October 1959.

22. Reissner, E., "A Note on Deflections of Plates on a Viscoelastic Foundation," Transactions, A.S.M.E., Vol. 25, No. 1, March 1958.

23. Pister, K. S., and Williams, M. L., "Bending of Plates on a Viscoelastic Foundation," Journal of the Engineering Mechanics Division, Proceedings, A.S.C.E., Vol. 86, No. EM 5, October 1960.

24. Pister, K. S., "Viscoelastic Plate on a Viscoelastic Foundation," Journal of the Engineering Mechanics Division, Proceedings, A.S.C.E., Vol. 87, No. EM 1, February 1961.

25. Monismith, C. L., and Secor, K. E., "Viscoelastic Behavior of Asphalt Concrete Pavements," Proceedings, International Conference on the Structural Design of Asphalt Pavements, University of Michigan, 1963.

26. Perloff, W. H., and Moavenzadeh, F., "Deflection of Viscoelastic Medium due to a Moving Load," Proceedings, International Conference on the Structural Design of Asphalt Pavements, University of Michigan, 1967.

27. Barksdale, R. D., and Leonards, G. A., "Predicting Performance of Bituminous Surfaced Pavements," Proceedings, International Conference on the Structural Design of Asphalt Pavements, University of Michigan, 1967.

28. Harr, M. E., "Influence of Vehicle Speed on Pavement Deflection," Proceedings, Highway Research Board, Vol. 41, 1962.

29. Roscoe, K. H., and Schofield, A. N., Discussion in Journal, Soil Mechanics and Foundation Section, American Society of Civil Engineers, January 1964.

30. Livneh, M. and Shklarsky, E., "The Bearing Capacity of Asphaltic Concrete Carpets," Proceedings, International Conference on the Structural Design of Asphalt Pavements, University of Michigan, 1962.

31. Puzinauskas, V. P., "Influence of Mineral Aggregate Structure on Properties of Asphalt Paving Mixtures," Highway Research Record No. 51, Highway Research Board, 1964.

32. Nevitt, H. G., "Compaction Fundamentals," Proceedings, Association of Asphalt Paving Technologists, Vol. 26, 1957.

33. Gaudette, N. G., Jr., "Application of the Kneading Compactor and Hveem Stabilometer to Bituminous Concrete Design in Indiana," Thesis submitted to Purdue University for MSCE degree, 1961 (unpublished).

34. Hearmon, R. F. S., An Introduction to Applied Anisotropic Elasticity, Oxford, London 1961.

35. Busching, H. W., "A Laboratory Investigation of Structural Design of Bituminous Mixtures," Ph.D. Thesis Submitted to Purdue University, 1967.

36. Truxal, J. C., Control System Synthesis, McGraw-Hill Book Co., 1955.

37. Nixon, F. E., Principles of Automatic Controls, Prentice Hall, Inc., 1960.

38. Goldberg, J. H., Automatic Controls: Principles of Systems Dynamics, Allyn & Bacon, Boston, 1964.

39. Tsien, H. S., Engineering Cybernetics, McGraw-Hill Book Co., 1954.

40. Etkin, B., Dynamics of Flight, John Wiley & Sons, 1959.

41. Crafton, P. A., Shock and Vibration in Linear Systems, Harper & Brothers, N. Y., 1961.

42. Busching, H. W., Goetz, W. H. and Harr, M. E., "Stress-Deformation Behavior of Anisotropic Bituminous Mixtures," Proceedings, AAPT, Vol. 36, 1967.

43. Papazian, H. S., "The Response of Linear Viscoelastic Materials in the Frequency Domain with Emphasis on Asphaltic Concrete," Proceedings, International Conference on the Structural Design of Asphalt Pavements, University of Michigan, 1962.

44. Lister, N. W., and Jones, R., "The Behavior of Flexible Pavements under Moving Wheel Loads," Proceedings, Second International Conference on the Structural Design of Asphalt Pavements, University of Michigan, 1967.

45. Pagen, C. A., "Rheological Response of Bituminous Concrete," Bituminous Materials and Mixes, Highway Research Record No. 67, Highway Research Board, 1965.

46. Kallas, B. F., and Riley, J. C., "Mechanical Properties of Asphalt Pavement Materials," Proceedings, Second International Conference on the Structural Design of Asphalt Pavements, University of Michigan, 1967.

APPENDIX

APPENDIX

TYPICAL EXAMPLE OF OBTAINING THE TRANSFER FUNCTION

Typical test results in a sinusoidal loading test on an asphaltic concrete specimen (z-1) at 80°F and the frequency response curves plotted from them are given in Table 10 and Fig. 20, respectively.

The first step is to approximate the frequency spectrum with asymptotes of slopes of six decibels per octave and to note the corner frequencies, as shown in Fig. 25 and Table 15.

TABLE 15

Slopes of Asymptotes and Corner Frequencies

Slope db/oct	Corner Frequency rad/sec
$k_1 = 0$	$\omega_1 = 0$
$k_2 = -6$	$\omega_2 = 0.02$
$k_3 = 0$	$\omega_3 = 0.025$
$k_4 = -6$	$\omega_4 = 0.1$
$k_5 = 0$	$\omega_5 = 0.2$
$k_6 = -6$	$\omega_6 = 1.0$
$k_7 = 0$	$\omega_7 = 2.0$
$k_8 = -6$	$\omega_8 = 10.0$

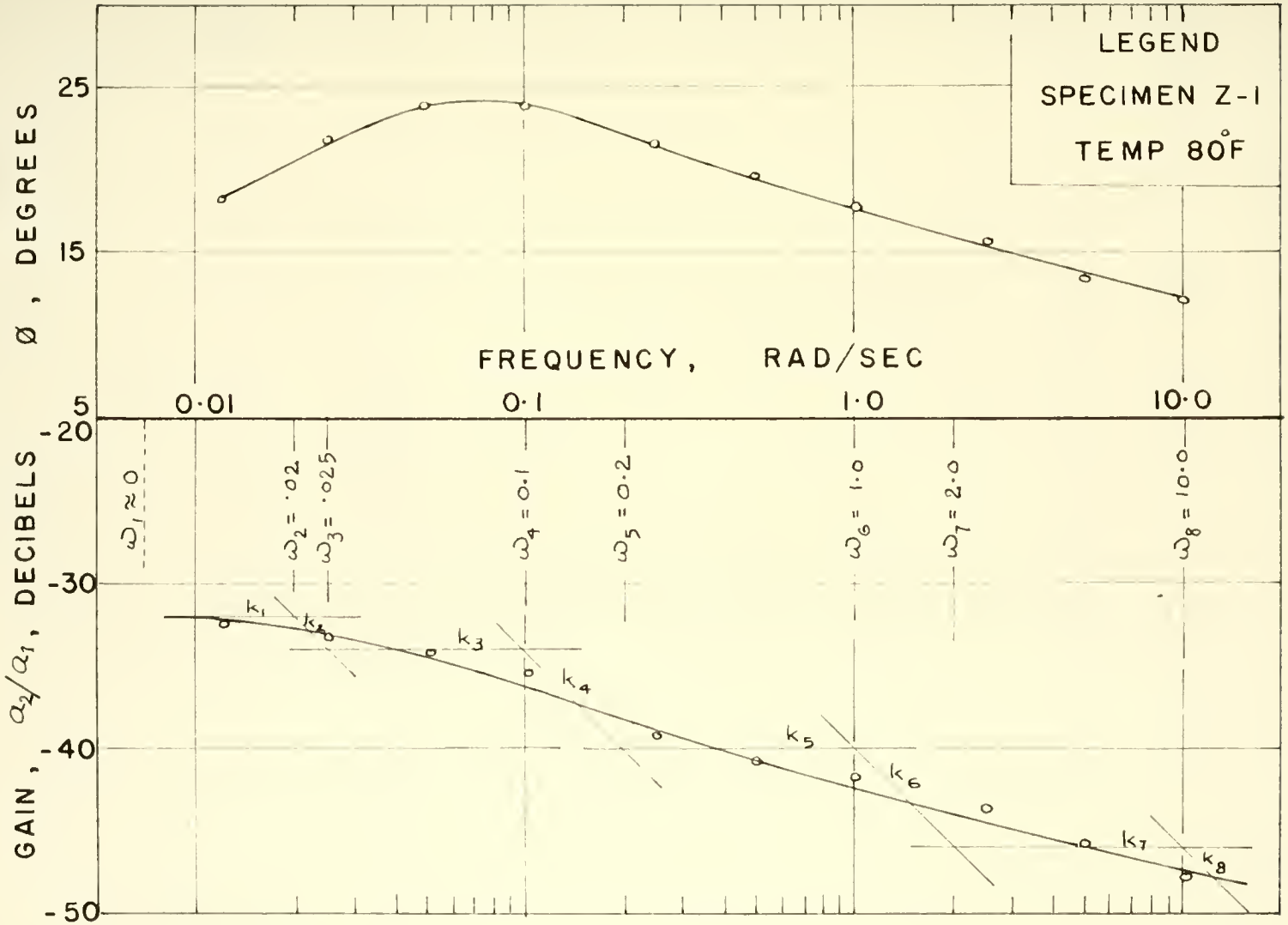

Fig. 25. Asymptotic approximation of the frequency spectrum

The approximate modified transfer function was seen to be

$$G(j\omega) = A(j\omega + \omega_1)^{\frac{k_1}{6}} (j\omega + \omega_2)^{\frac{k_2-k_1}{6}} \ldots (j\omega + \omega_n)^{\frac{k_n-k_{n-1}}{6}} \qquad (28)$$

Substituting the values from Table 15 in Eqn. 28, we get

$$G(j\omega) = \frac{A(j\omega + 0.025)(j\omega + 0.2)(j\omega + 2.0)}{(j\omega + 0.02)(j\omega + 0.1)(j\omega + 1.0)(j\omega + 10.0)} \qquad (58)$$

and the transfer function is accordingly

$$G(s) = \frac{A(s + 0.025)(s + 0.2)(s + 2.0)}{(s + 0.02)(s + 0.1)(s + 1.0)(s + 10.0)} \qquad (59)$$

where the constant A is determined at one experimental frequency as shown below.

A frequency in the spectrum is chosen at which the experimental curve and a horizontal asymptote intersect - such as $\omega = 0.4$ rad/sec in the present case. From Eqn. 58, the absolute value of the transfer function is obtained, by virtue of the property of a complex number, as

$$|G(j\omega)| = \frac{A(\omega^2 + 0.000625)^{1/2}(\omega^2 + 0.04)^{1/2}(\omega^2 + 4.0)^{1/2}}{(\omega^2 + 0.0004)^{1/2}(\omega^2 + 0.01)^{1/2}(\omega^2 + 1)^{1/2}(\omega^2 + 100)^{1/2}} \qquad (60)$$

Substituting for $\omega = 0.4$ in Eqn. 60, and evaluating we obtain

$$|G(j\omega)|_{\omega = 0.4} = 0.204\ A \qquad (61)$$

From Fig. 25 the value of the gain at $\omega = 0.4$ rad/sec is read as - 40.0 decibels; that is experimentally

$$\frac{a_{output}}{a_{input}} = \text{gain} = -40.0 \text{ db} \qquad (62)$$

Converting Eqn. 61 to decibel units and equating it to Eqn. 62,

$$20 \log_{10}(0.204A) = -40.0 \qquad (63)$$

Solving for A in Eqn. 63, A is obtained as a dimensionless constant,

$$A = 0.05 \qquad (64)$$

Substituting for A in Eqn. 59, the transfer function is obtained, as

$$G(s) = \frac{(0.05)(s + 0.025)(s + 0.2)(s + 2.0)}{(s + 0.02)(s + 0.1)(s + 1.0)(s + 10.0)} \qquad (65)$$

VITA

VITA

Shanmugam Arumuga Swami was born on May 30, 1928 in Sivakasi, Madras State, India. He attended the S.H.N.V. Elementary and High Schools in Sivakasi (1945). He received his Bachelor of Engineering degree from the Madras University, India, with First Class Honors in the year 1951.

After graduation, the author was employed as a Junior Engineer in the Highway Department of Madras State, India, for about a year after which he joined the College of Engineering, Guindy, Madras, as a research assistant and subsequently as a member of the Faculty.

In April 1956, the author joined the Central Road Research Institute, New Delhi, India, as a Senior Scientific Officer and worked in the Flexible Pavements and Bituminous Materials Division. In December 1959, he went to Australia under a Colombo Plan Scholarship and received his degree of Master of Technology in Highway Engineering from the University of New South Wales, Sydney (1961). Returning to India in 1961, he continued working in the C.R.R.I., New Delhi, until June 1964.

In September 1964, the author came to the United States of America to pursue his studies toward the Ph.D. at Purdue University in highway materials.

He has to his credit eight technical papers published in England, Australia and India.

Mr. Swami is married and is a citizen of India.